ROYAL SOCIETY OPEN SCIENCE

royalsocietypublishing.org/journal/rsos

Research

Cite this article: Pradelli LA, Pol D, Vega NA, Ezcurra MD. 2026 The axial osteology of the theropod dinosaur *Piatnitzkysaurus floresi* from the Early Jurassic of Patagonia, Argentina. *R. Soc. Open Sci.* **13**: 251876.
https://doi.org/10.1098/rsos.251876

Received: 13 October 2025
Accepted: 8 December 2025

Subject Category:
Earth and environmental science

Subject Areas:
palaeontology

Keywords:
Averostra, *Piatnitzkysaurus*, Piatnitzkysauridae, Tetanurae, Toarcian, vertebrae, tooth replacement

Authors for correspondence:
Luciano A. Pradelli
e-mail: lucianopradelli@gmail.com
Martín D. Ezcurra
e-mails: m.d.ezcurra@bham.ac.uk; martindezcurra@yahoo.com.ar

The axial osteology of the theropod dinosaur *Piatnitzkysaurus floresi* from the Early Jurassic of Patagonia, Argentina

Luciano A. Pradelli[1,2], Diego Pol[1,2], Nahuel A. Vega[3] and Martín D. Ezcurra[1,4]

[1]Sección Paleontología de Vertebrados, CONICET-Museo Argentino de Ciencias Naturales 'Bernardino Rivadavia', Buenos Aires, Argentina
[2]Facultad de Ciencias Exactas y Naturales, Universidad de Buenos Aires, Buenos Aires, Argentina
[3]Comisión Nacional de Energía Atómica (CNEA), Buenos Aires, Argentina
[4]School of Geography, Earth and Environmental Sciences, University of Birmingham, Birmingham, UK

LAP, 0009-0007-6761-5594; DP, 0000-0002-9690-7517; MDE, 0000-0002-6000-6450

Piatnitzkysaurus floresi is a theropod dinosaur from the Lower Jurassic deposits of the Cañadón Asfalto Formation of the Chubut Province, Patagonia, Argentina. This species is known from two specimens and is one of the few Early Jurassic tetanurans recorded worldwide. The braincase and the frontal were redescribed in detail, but the rest of the skull elements (two maxillae and a dentary) and the vertebrae have only been briefly described and illustrated in the original description of the species almost 40 years ago. In the present work, we reinterpret certain attributes of the braincase and redescribe in detail the preserved tooth-bearing bones and vertebral column of *Piatnitzkysaurus floresi*. Computed tomography scans of one of the maxillae and the dentary improve our knowledge about dental development in early tetanurans. We also emend the diagnosis of *Piatnitzkysaurus floresi* based on the redescription carried out here and in a previous study. The new information about *Piatnitzkysaurus floresi* improves our knowledge about the evolution of early averostrans and will provide useful data for phylogenetic analyses on the origins and early diversification of Tetanurae, the most ecomorphologically diverse clade of theropods.

THE ROYAL SOCIETY PUBLISHING

1. Introduction

The axial skeleton is one of the anatomical regions that underwent extensive modifications through the evolution of the theropod dinosaurs. Highly specialized and unique morphologies are present in this region of the skeleton among several averostran theropod groups, including ceratosaurians and carcharodontosaurids [1,2]. In order to reconstruct the sequence of acquisition of these specialized morphologies within Theropoda, it is crucial to understand the anatomy of the earliest known averostran taxa, including both ceratosaurs and tetanurans. In turn, Tetanurae represents the most diverse clade of theropod dinosaurs, comprising the major groups Allosauroidea, Megalosauroidea and Coelurosauria [3–10]. The oldest currently known averostrans are the Early Jurassic ceratosaurs *Berberosaurus liassicus* from Morocco, *Saltriovenator zanellai* from Italy and *Eoabelisaurus mefi* from Argentina [11–13], and the tetanurans *Asfaltovenator vialidadi*, *Condorraptor currumili* and *Piatnitzkysaurus floresi* [14–16]. The latter four taxa were found at the Toarcian fossiliferous levels of the Cañadón Asfalto Formation, Patagonia, Argentina [17–19]. Consequently, a detailed knowledge of these early tetanurans is essential for clarifying the phylogenetic relationships among the major clades of this group.

Among the earliest known averostran species, *Piatnitzkysaurus floresi* is one of the most complete, and the only one represented by two specimens (holotype: PVL 4073; referred specimen: MACN-Pv CH895). This species was initially described briefly by Bonaparte [14,20], but more recently the braincase and left frontal were redescribed in detail by Rauhut [21], and the appendicular osteology by Pradelli *et al.* [22]. In the present contribution, we provide the detailed redescription of *Piatnitzkysaurus floresi* through a revision of its axial, cranial and postcranial skeleton, and an updated emended diagnosis of this species. Our study also incorporates the analysis of micro-computed tomography scans of the dentary of the holotype and the maxilla of the referred specimen, yielding novel data still uncommonly available among Early Jurassic theropods [23,24]. A comprehensive redescription of *Piatnitzkysaurus floresi* is thus fundamental for improving our understanding of the early radiation of averostrans, particularly within Tetanurae, in the broader context of the break-up of Gondwana, and it provides critical anatomical information for future phylogenetic and macroevolutionary analyses.

2. Material and methods

As was previously mentioned, *Piatnitzkysaurus floresi* is known from two specimens. The holotype is housed at the Colección de Paleovertebrados of the Instituto Miguel Lillo of the Universidad Nacional de Tucumán (PVL) in San Miguel de Tucumán, and the referred specimen at the Colección Nacional de Paleovertebrados of the Museo Argentino de Ciencias Naturales (MACN-Pv) in Buenos Aires. The axial skeleton and cranial remains of both specimens were studied and analysed firsthand for the purpose of this redescription. The mechanical re-preparation of the axial bones of the referred specimen and the dentary of the holotype was conducted by the first author at the MACN. Textured three-dimensional (3D) models of all axial bones of both specimens were generated through photogrammetry using the software Agisoft PhotoScan Professional v. 1.3.3 (Agisoft LLC, www.agisoft.com, 2017). The photographs to build the models and make the figures were taken with a digital camera (Nikon D3100) with a 14-megapixel sensor, using an 18–55 mm lens.

Measurements of the axial skeleton of *Piatnitzkysaurus floresi* are included in tables 1–6. Lengths lower than 15 cm were measured using an electronic digital calliper. Lengths greater than 15 cm were measured using a metal calliper. Measurements indicated with an asterisk (*) indicate incomplete or uncertain distances (should be considered minimum distances in most cases). A dash (—) indicates that the structure cannot be measured.

The maxilla of the referred specimen and the dentary of the holotype were scanned using a NIKON XT H 225 ST 2× X-ray micro-CT system at the Laboratorio Argentino de Haces de Neutrones, Comisión Nacional de Energía Atómica (Buenos Aires, Argentina). Scanning was performed at 195 kV with a 0.25 mm Sn filter, acquiring 2500 projections and achieving a voxel resolution of 88 µm. The resulting tomographic slices were processed, segmented and visualized in Avizo (version 2021, Visualisation Sciences Group).

2.1. Institutional abbreviations

CMNH, Cleveland Museum of Natural History, Cleveland, United States of America; MACN-Pv CH, Museo Argentino de Ciencias Naturales 'Bernardino Rivadavia', Colección Nacional de

Table 1. Measurements of the braincase of *Piatnitzkysaurus floresi* (PVL 4073). Measurements in cm.

	braincase (PVL 4073)
foramen magnum, maximum height	2.11
foramen magnum, maximum width	2.52
occipital condyle, maximum height	2.42
occipital condyle, maximum width	3.46
subcondylar recess, maximum height	2.78
basipterygoid recess, dorsoventral height	1.07
dorsal tympanic recess, dorsoventral height	1.37
ventral tympanic recess, dorsoventral height	1.27
basisphenoid recess, maximum anteroposterior length	3.16
basisphenoid recess, maximum lateral width	2.04
vestibular eminence, maximum dorsoventral height	3.44
vestibular eminence, maximum lateral width	2.78
internal carotids cavity, maximum length	1.17

Table 2. Measurements of skull elements of *Piatnitzkysaurus floresi* (PVL 4073 and MACN-Pv CH895). Measurements in cm. Measurements with an asterisk indicate incomplete or uncertain distances. A dash indicates that it is not preserved.

	left frontal (PVL 4073)	left maxilla (PVL 4073)	right maxilla (MACN-Pv CH895)	left dentary (PVL 4073)
maximum length	10	20.38* (without anteromedial process)	22.41* (without anteromedial process)	9.57*
anterior lateromedial width	1.5	—	—	—
posterior lateromedial width	5.26	—	—	—
maximum dorsoventral height	2	9.45*	8.29*	4.32
maximum lateromedial width	—	3.83 (including anteromedial process)	3.47 (including anteromedial process)	2.2
anteromedial process, anteroposterior length	—	4.15	4.33	—
ascending process, maximum width	—	2.5	2.88	—
maxillary fenestra, maximum length	—	—	2.71*	—

Paleovertebrados, Colección Chubut, Ciudad Autónoma de Buenos Aires, Argentina; MLP, Museo de La Plata, La Plata, Argentina; MPEF-PV, Museo Paleontológico Egidio Feruglio, Paleontología de Vertebrados, Trelew, Argentina; MUCPv-CH, Museo de la Universidad Nacional del Comahue, Colección El Chocón, Villa El Chocón, Argentina; PULR-V, Museo de Ciencias Naturales, Universidad Nacional de La Rioja, Vertebrados, La Rioja, Argentina; PVL, Paleontología de Vertebrados, Fundación Miguel Lillo, Universidad Nacional de Tucumán, San Miguel de Tucumán, Argentina; PVSJ, División Paleontología Vertebrados, Museo de Ciencias Naturales de la Universidad Nacional de San Juan, San Juan, Argentina.

3. Systematic palaeontology

Dinosauria Owen, 1842 [25] *sensu* Padian & May, 1993 [26]
Theropoda Marsh, 1881 [27] *sensu* Gauthier, 1986 [4]
Tetanurae Gauthier, 1986 [4] *sensu* Holtz *et al.*, 2004 [28]
Piatnitzkysauridae Bonaparte, 1979 [14]
Piatnitzkysaurus floresi Bonaparte [14]

Table 3. Measurements of the cervical vertebrae of *Piatnitzkysaurus floresi* (PVL 4073). Measurements in cm. A dash indicates that it is not preserved.

	atlas-axis (PVL 4073)	4th presacral vertebra (PVL 4073)	5th presacral vertebra (PVL 4073)	7th presacral vertebra (PVL 4073)
maximum anteroposterior length	10.45	11.87	—	—
maximum dorsoventral height	11.57	—	—	12.85
odontoid process, anteroposterior length	1.95	—	—	—
odontoid process, dorsoventral height	2.43	—	—	—
axial intercentrum, anteroposterior length	1.96	—	—	—
neural spine, anteroposterior length	2.05	—	—	—
neural spine, lateral width	2.54	—	—	—
transverse process, maximum lateral width	7.98	—	—	—
transverse process, maximum dorsoventral height	6.05	—	—	—
vertebral centre, anterior height	4.55	—	—	4.28
vertebral centre, posterior height	4.05	—	—	3.62
vertebral centre, anteroposterior length	7.9	6.94	7.92	8.81
vertebral centre, anterior lateral width	—	5.13	5.36	—
vertebral centre, posterior lateral width	—	—	5.28	—
prezygapophysis, width	—	3.23	3.2	—
postzygapophysis, width	—	2.48	2.07	—
parapophysis, width	—	—	2.28	2.79
centrodiapophyseal fossa, maximum length	—	—	—	1.48
postzygapophyseal centrodiapophyseal fossa, maximum length	—	—	—	2.62
neural spine, width	—	—	—	0.98

Holotype. PVL 4073: incomplete left maxilla, left frontal, anterior end of a left dentary with erupting teeth, partial braincase, 14 presacral vertebrae including axis, postaxial cervical and dorsal vertebrae, incomplete sacrum with four vertebrae, two anterior caudal vertebrae, fragments of ribs, almost complete left and right scapulae, right and part of the left coracoids, right humerus, left ulna, fragment of postacetabular process of the right ilium, left and right pubes, shaft and distal end of left and right ischia, femora, tibiae and fibulae, and some indeterminate fragments [22]. There is morphological evidence that precludes assigning, at least unambiguously, the isolated teeth of PVL 4073 to *Piatnitzkysaurus floresi* (see the following description).

Referred specimen. MACN-Pv CH895: incomplete right maxilla with erupting teeth, one dorsal and two caudal vertebral centra, a neural spine fragment, two posterior dorsal vertebrae, complete sacrum with five vertebrae (four of them are fused), rib fragments, right humerus, left ilium, ischial peduncle of another left ilium, proximal end of left and right pubes, proximal and distal end of right ischium, iliac peduncle and distal end of left ischium, left femur, left tibia, left metatarsals II, III and IV, left distal tarsals 3 and 4, and one partial phalanx [22].

Table 4. Measurements of the anterior-middle dorsal vertebrae of *Piatnitzkysaurus floresi* (PVL 4073). Measurements in cm. Measurements with an asterisk indicate incomplete or uncertain distances. A dash indicates that it is not preserved.

	approx. 1st dorsal vertebra (PVL 4073)	approx. 2nd dorsal vertebra (PVL 4073)	approx. 4th dorsal vertebra (PVL 4073)	approx. 7th dorsal vertebra (PVL 4073)
maximum dorsoventral height	15.97	—	17.82	18.7
maximum lateral width	19.11	—	—	—
neural spine, dorsal width	3.25	—	3.22	2.62
prezygapophysis, maximum length	3.52	—	3.39	—
postzygapophysis, maximum length	4.18	—	—	1.94
parapophysis, width	3.02	2.22	3.49	—
anterior pleurocoel, length	1.99	—	—	—
posterior pleurocoel, length	1.48	—	—	—
prezygapophyseal centrodiapophyseal fossa, maximum length	5.59	—	—	—
vertebral centre, maximum anterior height	5.04	5.38	6.01	—
vertebral centre, maximum anterior width	7.88	7.95	6.56	—
vertebral centre, maximum posterior height	5.93	—	5.65	6.14
vertebral centre, maximum posterior width	7.22	—	—	5.48
ventral keel, anteroposterior length	2.6	—	—	—
ventral keel, dorsoventral height	—	3.52	3.25	—

Occurrence. Cerro Cóndor South locality, 1 km west of the Farias house at Cerro Cóndor village, Chubut Province, Argentina. Upper levels of the Cañadón Asfalto Formation dated between 178.766 ± 0.092 and 178.070 ± 0.21 Ma, Toarcian, Early Jurassic [19].

Emended diagnosis. Piatnitzkysaurus floresi is a non-avian tetanuran theropod with the following character states that distinguish it from other theropods (autapomorphies indicated with an asterisk): maxilla with base of the ascending process strongly medially inflated, exceeding the rest of the inner surface of the bone*; maxillary fenestra with a straight, anteroposteriorly aligned ventral margin*; anterior end of the frontal ventrally flexed*; preotic pendant widens and projects occipitally*; mid-posterior dorsal vertebrae with two ventrally oriented hook-shaped projections located at the level of the hypantrum and ventromedial to the prezygapophyses, which articulate with pointed protuberances located lateral to the centropostzygapophyseal laminae (also present in *Condorraptor currumili*); first sacral centrum with a thickened anteroventral edge that extends ventrally beyond the rest of the bone*; iliac blade with vertical ridge on its lateral surface at level with the ischiatic peduncle (also present in *Monolophosaurus jiangi*); and distal tarsal 4 with a transversely broadening posterior end*.

4. Description

4.1. Skull

Braincase. The braincase (figure 1*a,b*; table 1) and left frontal (figure 1*c,d*; table 2) of *Piatnitzkysaurus floresi* were described in detail by Rauhut [21]. We agree with the interpretation and description of the structures of the left frontal, but we interpret some structures of the braincase differently. In the right lateral view, anterodorsally to the thick metotic strut that separates the lateral surface of the braincase

Table 5. Measurements of the middle-posterior dorsal vertebrae of *Piatnitzkysaurus floresi* (PVL 4073 and MACN-Pv CH895). Measurements in cm. Measurements with an asterisk indicate incomplete or uncertain distances. A dash indicates that it is not preserved.

	approx. 10th dorsal vertebrae (PVL 4073)	approx. 11th dorsal vertebra (PVL 4073)	posterior dorsal vertebra (MACN-Pv CH895)	posterior dorsal vertebra (MACN-Pv CH895)
maximum dorsoventral height	22.39	—	21.7	20.97*
maximum anteroposterior length	10.96	10.36	9.3	9.47
maximum lateral width	—	—	15.95	—
neural spine, dorsoventral height	11.05	—	9.69	8.56*
postzygapophysis, maximum length	2.26	—	2.06	2.31
prezygapophysis, maximum length	—	2.58	—	—
parapophysis, width	1.9	1.99	—	—
vertebral centre, maximum anterior height	7.38	7.85	6.51*	7.25*
vertebral centre, maximum anterior width	7.05	7.8	7.49	7.34*
vertebral centre, maximum posterior height	7.58	8.59	6.89	—
vertebral centre, maximum posterior width	7.51	7.93	6.3*	—
vertebral centre, anteroposterior length	7.54	7.03	7.28	8.17

Table 6. Measurements of the sacral and caudal vertebrae of *Piatnitzkysaurus floresi* (PVL 4073 and MACN-Pv CH895). Measurements in cm. Measurements with an asterisk indicate incomplete or uncertain distances. A dash indicates that it is not preserved.

	1st sacral vertebra (MACN-Pv CH895)	2nd–5th sacral vertebrae (MACN-Pv CH895)	anterior caudal vertebra (PVL 4073)	anterior caudal vertebra (PVL 4073)
maximum dorsoventral height	16.91*	—	—	—
maximum anteroposterior length	8.2*	28.16	—	—
prezygapophysis, maximum length	3.15	—	—	—
vertebral centre, maximum anterior height	10.01*	—	8.3	7.26
vertebral centre, maximum anterior width	9.14*	—	8.05	7.56
vertebral centre, maximum posterior height	7.54*	—	—	—
vertebral centre, maximum posterior width	6.65*	—	—	—
vertebral centre, anteroposterior length	7.9*	—	7.4	7.04

from the posterior one, we interpret a shallow depression as the columellar recess instead of the metotic foramen mentioned by Rauhut [21]. This depression projects from the metotic foramen to the

anterolateral surface of the paraoccipital process. The metotic foramen should be present posteriorly to the fenestra ovalis, but these openings cannot be distinguished from each other because the crista tuberalis that separates them seems broken. The crista prootica forms the preotic pendant ventrally, which is a posteriorly oriented structure usually present in neotheropods (e.g. *Allosaurus fragilis* [29]; *Carnotaurus sastrei*: MACN-Pv CH894; *Majungasaurus crenatissimus* [30]; *Sinraptor dongi* [31]; *Megapnosaurus rhodesiensis*: cast of QG1; *Viavenator exxoni* [32]) but it widens and projects more occipitally in *Piatnitzkysaurus floresi* than in other theropods that we are aware of. The braincase of *Piatnitzkysaurus floresi* is highly pneumatized, resembling the condition in most theropods. We interpret the dorsal tympanic recess as the depression covered by the preotic pendant. In this recess, there are pneumatic cavities and the entrance of the internal carotid (one on each side). Ventral to this recess is the ventral tympanic recess, and anterior to it is the basipterygoid recess, which is less extended. We agree with Rauhut [21] on the position of the exits of the cranial nerves V and VII.

In anteroventral view, at both lateral sides of the vestibular eminence of the endocranial cavity, the floccular recesses are developed as oval depressions. On the floor of the endocranial cavity is a median longitudinal ridge surrounded at each side by shallow grooves. On the pituitary fossa, we interpret the entrance of both internal carotids as the ventral larger cavity, in contrast to Rauhut [21], who interpreted this as a depression for the pituitary gland within the pituitary fossa. We consider the latter fossa as the cavity located between both exits of the cranial nerve VI. We agree with Rauhut [21] regarding the interpretation of the other structures of the braincase.

Maxilla. The left maxilla is preserved in the holotype (PVL 4073: figure 2; table 2), while the right maxilla is preserved in the referred specimen (MACN-Pv CH895: figure 3; table 2). Both lack the distal end of the ascending process and the bone that surrounds the maxillary sinuses. In addition, the holotype lacks the anteroventral margin of the bone, and the referred specimen a small portion of the posterior end, which should have contacted the jugal. In ventral view, the maxilla of the holotype is slightly convex laterally in the anterior half and slightly convex medially in the posterior half. This curvature is less pronounced in the referred specimen, but it is more poorly preserved and some regions have been glued together with resin.

In lateral view, the maxillary edge of the subnarial foramen is developed as a small, distinct notch at the mid-height of the anterior margin of the bone. The antorbital fossa extends over most of the lateral surface of the maxilla as a shallow, weakly rimmed depression. This fossa is usually well extended in non-coelurosaurian neotheropods (e.g. *Asfaltovenator vialidadi*: MPEF-PV 3440; *Ceratosaurus* spp. [33,34]; *Marshosaurus bicentesimus* [35]; *Masiakasaurus knopfleri* [36]; *Megalosaurus bucklandii* [37]; *Torvosaurus gurneyi* [38]; *Megapnosaurus rhodesiensis* [39]; *Zupaysaurus rougieri*: PULR-V 076), while in abelisauroids it is reduced (e.g. *Carnotaurus sastrei*: MACN-Pv CH894; *Majungasaurus crenatissimus* [30]). The inner surface of the lateral wall of the floor of the antorbital fenestra possesses two big foramina and a few small ones. Posterior to these excavations, there are at least three other smaller cavities towards the jugal facet. Outside of the antorbital fossa, the lateral surface of the maxilla is rough, similar to some averostrans (e.g. *Asfaltovenator vialidadi*: MPEF-PV 3440; *Eustreptospondylus oxoniensis* [40]; *Megalosaurus bucklandii* [37]; *Sinraptor dongi* [31]), but it is less pronounced than the rougher surfaces found in other averostrans (e.g. *Carnotaurus sastrei*: MACN-Pv CH894; *Ceratosaurus* spp. [33,34]; *Majungasaurus crenatissimus* [30]; *Torvosaurus gurneyi* [38]), and contrasts with the smoother surface of *Dilophosaurus wetherilli* [23]. Ventral to the edge of the antorbital fossa, the lateral surface of the maxilla has numerous foramina aligned parallel to the ventral margin of the bone and more foramina are present on the anterior process, similar to the condition in most non-coelurosaurian averostrans (e.g. *Asfaltovenator vialidadi*: MPEF-PV 3440; *Ceratosaurus* spp. [33,34]; *Eustreptospondylus oxoniensis* [40]; *Majungasaurus crenatissimus* [30]; *Marshosaurus bicentesimus* [35]; *Megalosaurus bucklandii* [37]; *Sinraptor dongi* [31]; *Torvosaurus gurneyi* [38]). In contrast, *Dilophosaurus wetherilli* and *Zupaysaurus rougieri* (PULR-V 076) [23] have fewer foramina anteriorly. A groove for articulation with the jugal is present posterodorsally on the posterior process.

A large sub-oval fossa is here interpreted as the maxillary fenestra and occurs anterior to the antorbital fenestra at the base of the ascending process, resembling the condition of other early tetanurans (e.g. *Allosaurus fragilis* [29]; *Asfaltovenator vialidadi*: MPEF-PV 3440; *Megalosaurus bucklandii* [37]; *Sinraptor dongi* [31]; *Torvosaurus gurneyi* [38]). However, the maxillary fenestra does not perforate the maxilla from side to side and has a straight, anteroposteriorly oriented ventral margin in *Piatnitzkysaurus floresi*. In contrast, in non-coelurosaurian neotheropods, this ventral margin is usually concave (e.g. *Asfaltovenator vialidadi*: MPEF-PV 3440; *Monolophosaurus jiangi* [41]; *Sinraptor dongi* [31]), only partially straight (e.g. *Allosaurus fragilis* [29]; *Marshosaurus bicentesimus* [35]), or straight and inclined (e.g. *Eustreptospondylus oxoniensis* [40]; *Megalosaurus bucklandii* [37]). The holotype possesses, anterior

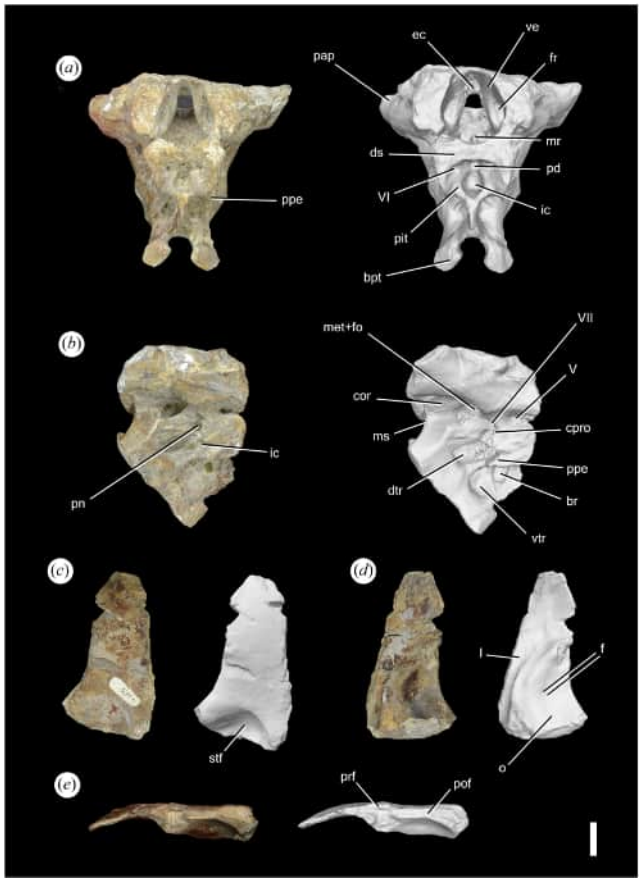

Figure 1. Photographs (left) and 3D models (right) of the braincase (*a,b*) and the left frontal (*c–e*) of PVL 4073 in (*a*) anteroventral, (*b*) right lateral, (*c*) dorsal, (*d*) ventral and (*e*) left lateral views. I, V, VI, VII, indicate foramina for the passage of cranial nerves; bpt, basipterygoid process; br, basipterygoid recess; cor, columellar recess; cpro, crista prootica; dtr, dorsal tympanic recess; ds, dorsum sellae; ec, endocranial cavity; f, foramina; fr, floccular recess; ic, entrance of internal carotids; met+fo, metotic + fenestra ovalis; mr, medial ridge of the endocranial cavity; ms, metotic strut; o, orbital facet; pap, paraoccipital process; pit, pituitary fossa; pd, depression for the pituitary gland within the pituitary fossa; pn, pneumatic pocket; pof, facet for the postorbital; ppe, preotic pendant; prf, facet for the prefrontal; stf, supratemporal fossa; ve, vestibular eminence; vtr, ventral tympanic recess. Scale bar equals 2 cm.

to the maxillary fenestra, a promaxillary foramen, which is also blind, but considerably smaller and shallower. Anterior to the promaxillary foramen is a relatively large pneumatic cavity that invades the anterior process of the maxilla at the level of the anteromedial process. This cavity is not visible externally because it is completely covered by thin layers of bone laterally and medially. However, the lateral bony wall is broken in the holotype, exposing this pneumatic recess in lateral and dorsal views (figure 2). This pneumatic recess is transversely expanded, producing a medial inflation of the maxilla in this region that is autapomorphic for *Piatnitzkysaurus floresi* [42] (although the condition is unknown in *Condorraptor currumili*). The dorsal surface of the maxilla in the transition between the anterior and ascending processes has a shallow groove for articulation with the nasal.

The medial surface of the maxilla is relatively smooth with faint striations. The anteromedial process (= palatal process) emerges medially from the anterior end. This process curved ventrally, being convex dorsally and anteroventrally oriented at its tip. It bears two longitudinal grooves that extend along the medial surface of the process, following its curvature. The dorsal groove is wider and deeper than the ventral one, but the dorsal one narrows anteriorly. The anteromedial process of the maxilla of *Piatnitzkysaurus floresi* resembles that of most tetanurans (e.g. *Allosaurus fragilis* [29]; *Eustreptospondylus oxoniensis* [40]; *Mapusaurus roseae* [6]; *Megalosaurus bucklandii* [37]; *Sinraptor dongi* [31]; *Torvosaurus gurneyi* [38]), while in *Dilophosaurus wetherilli* and *Zupaysaurus rougeri,* it is more anteriorly extended (PULR-V 076; [23]). A circular notch for the articulation with the premaxilla is present between the anterior and the anteromedial processes. There are two small foramina on the medial surface, posterodorsal to the anteromedial process, that pierce into a pneumatic sinus within the antorbital fossa (see below). There is a distinctly striated, shallowly depressed flat surface on the

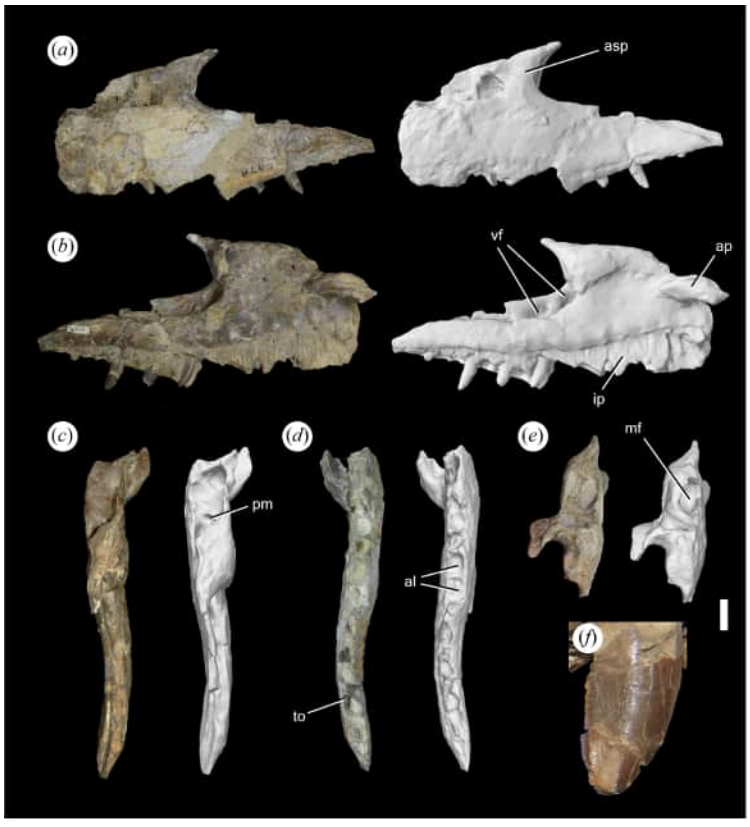

Figure 2. Photographs (left) and 3D model (right) of the left maxilla (*a–e*) of PVL 4073 in (*a*) lateral, (*b*) medial, (*c*) dorsal, (*d*) ventral and (*e*) anterior views. Close-up of maxillary emerging tooth in (*f*) lingual view. al, alveoli; ap, anteromedial process; asp, ascending process; ip, interdental plate; mf, maxillary fenestra; pm, promaxillary foramen; to, tooth; vf, vascular foramina. Scale bar equals 2 cm in (*a–e*) and (*f*) without scale.

medial surface of the maxilla between the eighth and thirteenth tooth positions. This facet is slightly anterodorsally to posteroventrally oriented and articulated with the palatine.

The alveoli are bounded medially by unfused interdental plates that are relatively tall and subpentagonal in shape, resembling the condition in some early tetanuran theropods (e.g. *Acrocanthosaurus atokensis* [43]; *Megalosaurus bucklandii* [37]; *Sinraptor dongi* [31]; *Torvosaurus gurneyi* [38]), although the plates are taller in *Megalosaurus bucklandii* [37]. These plates are similar to those in *Allosaurus fragilis*, even though they are fused in the latter [29]. The interdental plates are also usually fused in carcharodontosaurids (e.g. *Giganotosaurus carolini*: MUCPv-CH-1; *Mapusaurus roseae* [6]), ceratosaurians (e.g. *Carnotaurus sastrei*: MACN-Pv CH894; *Ceratosaurus* spp. [33,34]; *Majungasaurus crenatissimus* [30]) and *Torvosaurus gurneyi* [38]. The interdental plates bear dorsoventrally oriented striation, as in *Megalosaurus bucklandii* [37] and abelisaurids (e.g. *Carnotaurus sastrei*: MACN-Pv CH894; *Majungasaurus crenatissimus* [30]). Both alveoli and interdental plates decrease in anteroposterior length posteriorly in the dental series, and this is accompanied by a notable decrease in height of the interdental plates. Dorsal to the interdental plates, the bone widens medially from the third alveolus to the posterior end.

The maxilla has 18 tooth positions, more than in most other Jurassic averostrans (e.g. *Asfaltovenator vialidadi*: 13 tooth positions [16]; *Ceratosaurus* spp.: 12–15 tooth positions [33,34]; *Megalosaurus bucklandii*: 13–14 tooth positions [37]; *Sinraptor dongi*: 15 tooth positions [31]) and similar to *Allosaurus fragilis* (maximum of 16–17 tooth positions [29,33]), *Majungasaurus crenatissimus* (17 tooth positions [30]) and *Marshosaurus bicentesimus* (at least 16 tooth positions [35]). In contrast, non-averostran theropods usually have more tooth positions than in *Piatnitzkysaurus floresi* (e.g. *Coelophysis bauri*: 23 tooth positions [44]; *Megapnosaurus rhodesiensis*: 19–20 tooth positions [39]). In the holotype, eight teeth are preserved *in situ*; only two seem to have erupted, one almost complete (13th tooth position) and the other lacking the apex of the crown (11th tooth position). Four teeth started to erupt between the interdental plates, of which three have broken apices (4th, 6th and 14th tooth positions), and the other is fairly complete (9th tooth position). The remaining two teeth barely appear between the base of the interdental plates (3rd and 5th tooth positions). In the referred specimen, eleven teeth are

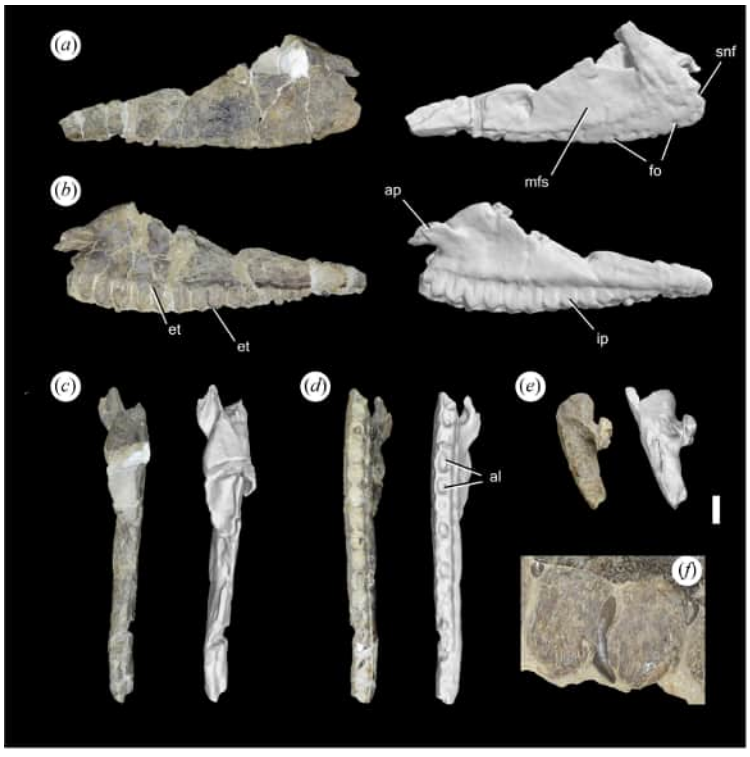

Figure 3. Photographs (left) and 3D model (right) of the right maxilla (*a*–*e*) of MACN-Pv CH895 in (*a*) lateral, (*b*) medial, (*c*) dorsal, (*d*) ventral and (*e*) anterior views. Close-up of maxillary emerging tooth in (*f*) lingual view. al, alveoli; ap, anteromedial process; et, emerging tooth; fo, foramina; ip, interdental plate; mfs, maxillary fossa; snf, subnarial foramen. Scale bar equals 2 cm in (*a*–*e*) and (*f*) without scale.

preserved *in situ*, but none are fully erupted. Four teeth have erupted but are broken at the base of the crown (3rd, 10th, 12th and 13th tooth positions). If they had remained complete, they would have been fully erupted. Two teeth are visible between the interdental plates (8th and 15th positions), and one of them has a broken crown apex. The remaining five teeth barely appear between the base of the interdental plates (1st, 3rd, 5th, 7th and 9th tooth positions). The position of these last five teeth indicates an alternate tooth replacement along the tooth row. The broken base of an erupted crown and an emerging tooth, between the base of the interdental plates, are present at the third tooth position.

The rendering of the maxilla of the referred specimen based on microCT-scan data (figure 4) supports the presence of 18 alveoli and allows evaluating the level of eruption of the teeth. The five teeth (1st, 3rd, 5th, 7th and 9th tooth positions) that are barely appearing at the base of the interdental plates observed with the unaided eye are actually emerging, and only the cusps of these teeth are visible. The position and maturity of these five teeth suggest an alternate replacement along the tooth row up to the 11th position. The last teeth of the tooth row do not seem to follow this maturity pattern. The most mature teeth with preserved cusps have a recurved crown. Unerupted teeth can be seen in all the tooth positions where no teeth are observed with the unaided eye (i.e. 2nd, 4th, 6th, 11th, 14th, 16th, 17th and 18th). There are at least two dental generations (i.e. with different maturity stages) coexisting in the same alveolus at the 3rd, 4th, 6th, 8th, 10th, 12th, 13th, 14th, 15th and 16th tooth positions, and three generations in 4th and 13th positions. The different generations vary from old, not yet completely reabsorbed roots that correspond to shed tooth crowns, emerged teeth and very immature, unerupted teeth. The most immature teeth in all positions are located lingually.

The anterior pneumatic cavity of the maxilla of the referred specimen can be identified through the micro-CT scan. This sinus resembles the condition seen in the holotype but is incomplete in the latter specimen. The pneumatic sinus in the referred maxilla is globose, subconical in shape and has two shallow ventral depressions that seem to coincide with the location of the promaxillary foramen and more anteriorly with the anteromedial process. The facet for the articulation with the jugal is anteroposteriorly extended and is U-shaped. It becomes shallower posteriorly.

Dentary. The anterior end of the left dentary is preserved in the holotype (PVL 4073; figure 5; table 2). The dentary preserves nine tooth positions and has three erupting teeth *in situ*. No fully erupted teeth are present. A well-preserved erupting tooth is present in the 7th position, while the

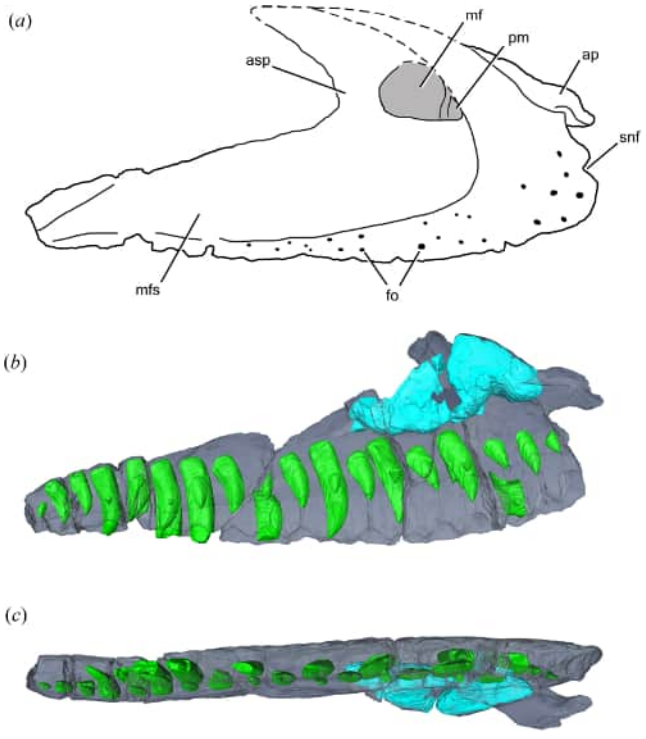

Figure 4. (*a*) Schematic line drawing of the reconstruction of the right maxilla of *Piatnitzkysaurus floresi* based on the holotype (PVL 4073) and the referred specimen (MACN-Pv CH895) in lateral view. (*b*,*c*) Rendering of the right maxilla of MACN-Pv CH895 in (*b*) lateral and (*c*) ventral views. ap, anteromedial process; asp, ascending process; fo, foramina; mf, maxillary fenestra; mfs, maxillary fossa; pm, promaxillary foramen; snf, subnarial foramen. Teeth are coloured in green; pneumatic cavities in cyan; and bone in grey.

other more exposed tooth is in the 2nd position, which is missing the apex of the crown. Only the apex emerges from a third tooth in the 5th position. Based on the short preserved portion of the bone and compared to the length of the maxilla, it is estimated that many alveoli are missing. The dentary is proportionally dorsoventrally low, with subparallel dorsal and ventral margins. It is transversely compressed and less robust than in ceratosaurians (e.g. *Carnotaurus sastrei*: MACN-Pv CH894; *Ceratosaurus dentisulcatus* [34]; *Majungasaurus crenatissimus* [30]; the Ceratosauridae indet. MPEF-PV 6775 from the Cañadón Asfalto Formation [24]), but more robust than in non-averostran neotheropods (e.g. *Dilophosaurus wetherilli* [23]; *Panguraptor lufengensis* [45]; *Megapnosaurus rhodesiensis* [39]), resembling the condition in several early tetanurans (e.g. *Allosaurus fragilis* [29]; *Asfaltovenator vialidadi*: MPEF-PV 3440; *Megalosaurus bucklandii* [37]; *Sinraptor dongi* [31]). The dentary has an angular anteroventral margin similar to *Mapusaurus roseae* [6], while this margin is more rounded in most other early neotheropods (e.g. *Allosaurus fragilis* [29]; *Asfaltovenator vialidadi*: MPEF-PV 3440; *Carnotaurus sastrei*: MACN-Pv CH894; *Ceratosaurus dentisulcatus* [34]; *Dilophosaurus wetherilli* [23]; *Majungasaurus crenatissimus* [30]; *Monolophosaurus jiangi* [46]; the Ceratosauridae indet. MPEF-PV 6775 [24]; *Sinraptor dongi* [31]) and more angular in most carcharodontosaurids (e.g. *Giganotosaurus carolini*: MUCPv-CH-1; *Tyrannotitan chubutensis*: MPEF-PV 1156). A small but distinct anteroventral process is present at the anteroventral corner of the bone, which is reminiscent of the condition in carcharodontosaurids (e.g. *Giganotosaurus carolini*: MUCPv-CH-1; *Mapusaurus roseae* [6]; *Tyrannotitan chubutensis*: MPEF-PV 1156).

In dorsal view, the alveoli are subcircular and separated from each other by thin septa, except the first two tooth positions that are continuous, although the septum could be broken. On the lateral surface, there are many foramina on the anterior region of the dentary, as in most theropods. These foramina are arranged in longitudinal rows, as in *Allosaurus fragilis* [29] and *Monolophosaurus jiangi* [46], while many averostrans have a row of foramina associated with a longitudinal lateral sulcus (e.g. *Ceratosaurus* spp. [33,34]; *Genyodectes serus*: MLP 26–39; *Giganotosaurus carolini*: MUCPv-CH-1; *Majungasaurus crenatissimus* [30]; *Megalosaurus bucklandii* [37]; *Sinraptor dongi* [31]). In contrast, there is no lateral sulcus, at least in the preserved portion of the dentary of *Piatnitzkysaurus floresi*. The foramina are arranged in two dorsal and one ventral longitudinal rows.

In medial view, the Meckelian groove extends anteriorly up to the level of the third tooth position. The Meckelian groove is shallow posteriorly and becomes deeper and wider at the level of the fourth

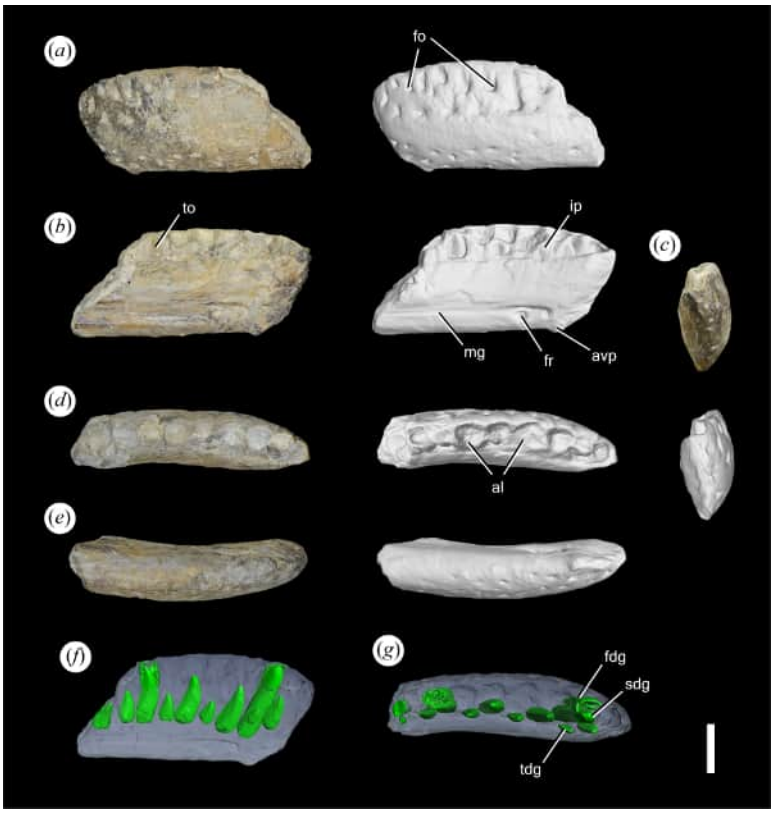

Figure 5. Photographs (left/above) and 3D model (right/below) (*a–e*) and rendering (*f,e*) of the left dentary of PVL 4073 in (*a*) lateral, (*b,f*) medial, (*c*) anterior, (*d,g*) dorsal and (*e*) ventral views. al, alveoli; avp, anteroventral process; fdg, first dental generation; fo, foramina; fr, foramen; ip, interdental plate; mg, Meckelian groove; sdg, second dental generation; tdg, third dental generation; to, tooth. Scale bar equals 2 cm. Teeth are coloured in green, and the bone in grey.

tooth position. This groove is positioned on the ventral third of the dentary and finishes in an oval foramen. Another foramen is associated ventral to the groove at the level of the fourth tooth position. Two foramina associated with the Meckelian groove are usual among tetanuran theropods and some ceratosaurians (e.g. *Allosaurus fragilis* [29]; *Asfaltovenator vialidadi*: MPEF-PV 3440; *Ceratosaurus* spp. [33,34]; *Megalosaurus bucklandii* [37]; *Monolophosaurus jiangi* [46]; *Sinraptor dongi* [31]). The interdental plates are barely preserved and seem to be sub-pentagonal in shape without signs of fusion, as in many non-coelurosaurian tetanurans (e.g. *Asfaltovenator vialidadi*: MPEF-PV 3440; *Megalosaurus bucklandii* [37]; *Monolophosaurus jiangi* [46]; *Sinraptor dongi* [31]), contrasting with the interdental plates fused to each other in the maxilla and/or dentary of *Allosaurus fragilis* [29], carcharodontosaurids (e.g. *Giganotosaurus carolini*: MUCPv-CH-1; *Mapusaurus roseae* [6]) and most ceratosaurians (e.g. *Carnotaurus sastrei*: MACN-Pv CH894; *Eoabelisaurus mefi*: MPEF-PV 3390; *Genyodectes serus*: MLP 26-39; *Majungasaurus crenatissimus* [30]; *Noasaurus leali*: PVL 4061). The anterior end of the dentary is D-shaped in anterior view, with a flat medial surface and a convex lateral one. The latter surface bears numerous small foramina. The large foramen present anterior to the tooth row in *Asfaltovenator vialidadi* (MPEF-PV 3440) and the Ceratosauridae indet. MPEF-PV 6775 [24] is absent in *Piatnitzkysaurus floresi*. The symphysis extends dorsoventrally across the complete height of the dentary and is restricted to the anteriormost portion of the bone. The symphyseal surface is faintly striated.

The rendering of the dentary of the holotype based on the microCT-scan data (figure 5) supports the presence of at least nine tooth positions mentioned in the previous description. There are teeth present in all the tooth positions. Other than the three teeth mentioned in the description (positions 2nd, 5th and 7th), the tooth in the 3rd position has a similar maturity state as the one in the 5th position. At least two tooth generations coexist in the same alveolus at the tooth positions 2nd, 7th and 9th. Old roots, not yet reabsorbed, are present labially in the positions 2nd and 7th, while in position 2nd, there is an early immature tooth located lingually. Both teeth are broken in position 9, and the most immature is located lingually. As in the first 11 positions of the maxilla, the location and the maturity of all the teeth in the dentary suggest an alternate tooth replacement along the tooth row.

Teeth. The tooth crowns are elliptical in cross-section, labiolingually compressed and have serrated mesial and distal carinae. The crowns are apicobasally tall, as in some non-coelurosaurian tetanurans (e.g. *Allosaurus fragilis* [29]; *Asfaltovenator vialidadi*: MPEF-PV 3440; *Sinraptor dongi* [31]; megalosauroids [47]), but they are taller in ceratosaurids (e.g. *Ceratosaurus* spp. [33,34]; *Genyodectes serus*: MLP 26–39). In contrast, the tooth crowns are shorter in abelisaurids (e.g. *Majungasaurus crenatissimus* [30]; *Spectrovenator ragei* [48,49]). The distal carina seems to reach the base in all the preserved crowns, both in the maxilla and dentary, which is usual in averostrans (e.g. *Allosaurus fragilis* [29]; *Asfaltovenator vialidadi*: MPEF-PV 3440; *Genyodectes serus*: MLP 26–39; *Majungasaurus crenatissimus* [30]; *Torvosaurus gurneyi* [38]). In the dentary, the mesial carina appears to reach the base of the crown in all teeth, but none is fully erupted. In the maxilla, all teeth that are not fully erupted or only the apex is visible have their mesial carina extending basally more than halfway down the crown, resembling the condition in megalosauroids and abelisauroids [50]. The mesial denticles become mesiodistally shorter towards the base and, thus, it can be difficult to distinguish the end of the carina. The mesial carina is slightly twisted lingually towards the base of the crown, and it is more restricted apically in *Condorraptor currumili* (MPEF-PV 1695).

The distal denticles are chisel-like, while the mesial ones are chisel-like to subquadrangular. The mesial denticles are flatter in the dentary than in the maxilla and flatten towards the base in both cases. There are approximately 16–17 denticles per 5 mm on both carinae, resembling the condition in *Condorraptor currumili* (MPEF-PV 1695). In contrast, early ceratosaurians (e.g. *Eoabelisaurus mefi*, 10 mesial denticles per 5 mm: MPEF-PV 3990; *Genyodectes serus*, 12 denticles per 5 mm [51]; the Ceratosauridae indet. MPEF-PV 6775, 12–13 denticles per 5 mm [24]; *Saltriovenator zanellai*, 12 denticles per 5 mm [12]) and *Asfaltovenator vialidadi* (12–13 denticles per 5 mm; MPEF-PV 3440) have fewer denticles per 5 mm. The density of the denticles is slightly greater near the base. 'Blood grooves' (narrow grooves continuing onto the crown from between the denticles), interdenticular sulci, and wrinkles are absent in all preserved crowns. The enamel has a rugose surface on both labial and lingual sides that is not clearly visible with the unaided eye, similar to the condition in some early averostran neotheropods (*Asfaltovenator vialidadi*: MPEF-PV 3440; *Eoabelisaurus mefi*: MPEF-PV 3990; the Ceratosauridae indet. MPEF-PV 6775 [24]; *Torvosaurus gurneyi* [38]).

Most of the referred isolated teeth (MACN-Pv CH895) probably do not belong to *Piatnitzkysaurus floresi*. These teeth have 12–14 denticles per 5 mm (both mesially and distally), and they are much larger than those of the currently known specimens of *Piatnitzkysaurus floresi*. In addition, the mesial carina does not reach half down the crown. The morphology of these teeth suggests that they could belong to *Asfaltovenator vialidadi* or an unknown species. There is only one referred tooth that could belong to *Piatnitzkysaurus floresi*, which has 13–15 denticles per 5 mm and is smaller and narrower labiolingually than the other referred teeth. This tooth has a mesial carina, but only the base is preserved, and it has a size that matches that of the largest maxillary teeth of *Piatnitzkysaurus floresi*.

In addition to the teeth preserved *in situ* in the left maxilla and dentary, there are three isolated teeth preserved in the holotype (PVL 4073). These teeth include one almost complete crown, one crown with a partial root, and the base of a crown with the root. Although these teeth have a size and density of denticles similar to those of the maxillary teeth, they possess 'blood grooves', which are not present in any *in situ* teeth in the preserved maxillae (left maxilla from the holotype and right one from the referred specimen) and dentary (from the holotype). In this study, due to this difference, these isolated teeth are not considered to belong to *Piatnitzkysaurus floresi*.

4.2. Vertebral column

The terminology used here to describe the laminae and associated fossae of the vertebrae follows that proposed for sauropods and other saurischian dinosaurs by Wilson [52] and Wilson *et al.* [53].

Atlas-axis. The atlantal pleurocentrum (hereafter called centrum for simplicity), the axial intercentrum and the axis are preserved in the holotype (PVL 4073: figure 6; table 3). The atlantal centrum is subconical, with an anteriorly facing apex, and is surrounded by a subcircular shallow fossae ventrally and laterally. The atlantal centrum is fused to the axis, forming an odontoid process, as is common in theropods (e.g. *Allosaurus fragilis* [29]; *Asfaltovenator vialidadi*: MPEF-PV 3440; *Carnotaurus sastrei*: MACN-Pv CH894; *Majungasaurus crenatissimus* [1]; *Dilophosaurus wetherilli* [23]) and herrerasaurids (e.g. *Herrerasaurus ischigualastensis* [54]; *Sanjuansaurus gordilloi* [55]). The dorsal surface of the odontoid process is transversely concave, where the spinal cord passes through the neural canal. The axial intercentrum is also fused to the axis, but an irregular surface with shallow depressions and low

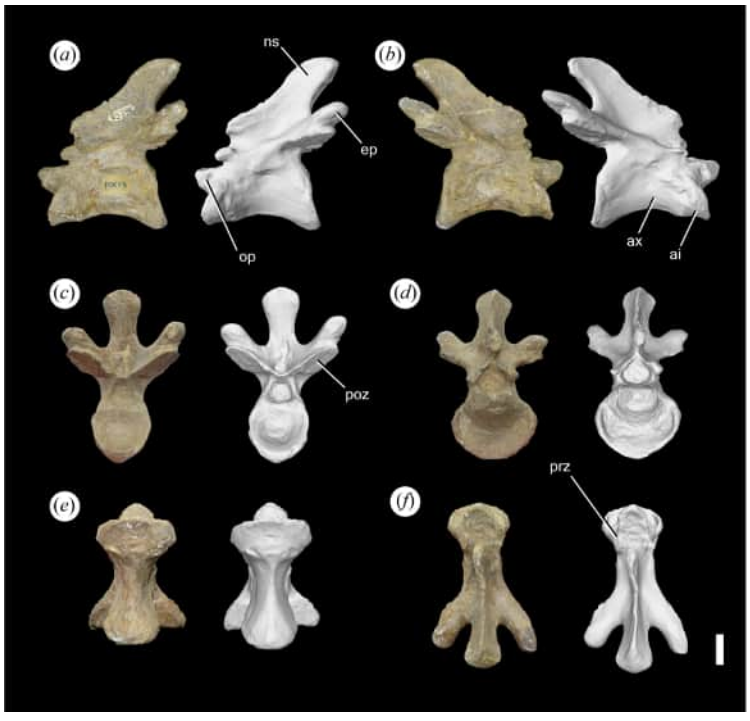

Figure 6. Photographs (left) and 3D model (right) of the atlantal centrum, axial intercentrum and axis of PVL 4073 in (*a*) left lateral, (*b*) right lateral, (*c*) posterior, (*d*) anterior, (*e*) ventral and (*f*) dorsal views. ai, axial intercentrum; axe, axis; ep, epipophysis; ns, neural spine; op, odontoid process; poz, postzygapophysis; prz, prezygapophysis. Scale bar equals 2 cm.

mounds allows identifying the boundaries between the elements. The axial intercentrum is triangular in lateral view, with a broad ventral surface and has a thickened margin surrounding the concave anterior surface, which extends slightly ventrally. The axial intercentrum has a posterolaterally facing small depression at mid-height on both lateral faces. The ventral margin of the axial intercentrum is almost straight in lateral view, contrasting with the dorsally arched ventral margin of the axial centrum.

The ventral surface of the axial centrum has a low longitudinal keel, but it is less developed than in other tetanurans (e.g. *Allosaurus fragilis* [29]; *Monolophosaurus jiangi* [56]; *Sinraptor dongi* [31]) and non-averostran saurischians (e.g. *Dilophosaurus wetherilli* [23]; *Gnathovorax cabreirai* [57]; *Herrerasaurus ischigualastensis* [54]; *Leonerasaurus taquetrensis* [58]). In ventral view, the anterior margin of the centrum is wider than the posterior one, as in allosauroids (e.g. *Allosaurus fragilis* [29]; *Asfaltovenator vialidadi*: MPEF-PV 3440; *Sinraptor dongi* [31]) and *Herrerasaurus ischigualastensis* [54]. In contrast, the anterior and posterior margins of the axial centrum are subequal in width in *Dilophosaurus wetherilli* [23]. Besides, the centrum is slenderer transversely in *Piatnitzkysaurus floresi* than in *Allosaurus fagrilis* [29], resembling the condition in *Dilophosaurus wetherilli* [23], *Herrerasaurus ischigualastensis* [54] and *Megapnosaurus rhodesiensis* [39]. The posterior surface of the axial centrum is strongly concave and delimited by a thickened edge.

The neural canal has sub-circular anterior and posterior openings. The prezygapophyses are short and possess a dorsolaterally facing articular facet. The postzygapophyses are subquadrangular with a mainly ventrally facing articular facet. On the dorsal surface of each postzygapophysis is a pointed epipophysis, which have a rounded end and are connected to the neural spine by a low spinopostzygapophyseal lamina, resulting in a prominent notch between the epipophysis and the neural spine in posterior view, as is usual in early tetanurans (e.g. *Allosaurus fragilis* [29]; *Concavenator corcovatus* [59]; *Mapusaurus roseae* [6]; *Monolophosaurus jiangi* [56]). In contrast, in non-tetanuran saurischians (e.g. *Carnotaurus sastrei*: MACN-Pv CH894; *Ceratosaurus dentisulcatus* [34]; *Dilophosaurus wetherilli* [23]; *Herrerasaurus ischigualastensis* [54]; *Megapnosaurus rhodesiensis* [39]), this lamina is more dorsally extended. The epipophyses are less dorsally oriented and more posteriorly projected than in *Dilophosaurus wetherilli* [23] and ceratosaurians (e.g. *Carnotaurus sastrei*: MACN-Pv CH894; *Ceratosaurus dentisulcatus* [34]; *Majungasaurus crenatissimus* [1]), resembling the condition in *Allosaurus fragilis* [29]. The epipophyses extend posteriorly beyond the postzygapophyses more than in *Allosaurus fragilis* [29]. The neural spine rises anterodorsally from the roof of the neural canal and projects posterodorsally

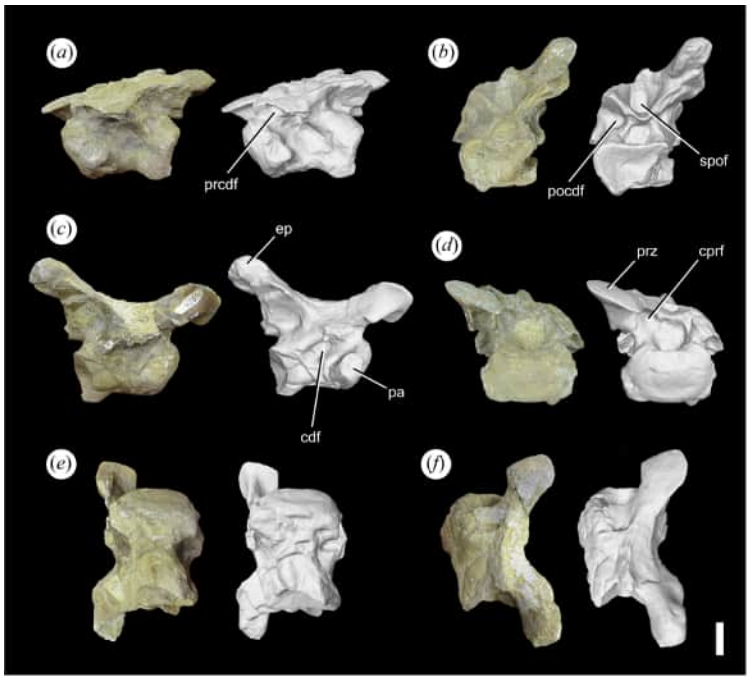

Figure 7. Photographs (left) and 3D model (right) of the fourth cervical vertebra of PVL 4073 in (*a*) left lateral, (*b*) posterior, (*c*) right lateral, (*d*) anterior, (*e*) ventral and (*f*) dorsal views. cdf, centrodiapophyseal fossa; cprf, centroprezygapophyseal fossa; ep, epipophysis; pa, parapophysis; pocdf, postzygapophyseal centrodiapophyseal fossa; prcdf, prezygapophyseal centrodiapophyseal fossa; prz, prezygapophysis; spof, spinopostzygapophyseal fossa. Scale bar equals 2 cm.

to beyond the level of the postzygapophyses. The neural spine is low and bulbous anteriorly, and it becomes taller and thinner posteriorly, a similar condition to that of other averostrans (e.g. *Allosaurus fragilis* [29]; *Majungasaurus crenatissimus* [1]; *Monolophosaurus jiangi* [56]; *Yunyangosaurus puanensis* [60]). In contrast, the neural spine is anteriorly taller and dorsally convex in some non-tetanuran theropods (e.g. *Carnotaurus sastrei*: MACN-Pv CH894; *Ceratosaurus dentisulcatus* [34]; *Dilophosaurus wetherilli* [23]; *Limusaurus inextricabilis* [61]).

No pleurocoels are present in the axis of *Piatnitzkysaurus floresi*, contrasting with their presence in several averostrans (e.g. *Allosaurus fragilis* [29]; *Carnotaurus sastrei*: MACN-Pv CH894; *Eustreptospondylus oxoniensis* [40]; *Monolophosaurus jiangi* [56]; *Sinraptor hepingensis* [62]). *Piatnitzkysaurus floresi* lacks the fossa present ventral to the diapophysis in ceratosaurians (e.g. *Carnotaurus sastrei*: MACN-Pv CH894; *Ceratosaurus dentisulcatus* [34]; *Majungasaurus crenatissimus* [1]).

Post-axial cervical vertebrae. The probable fourth, fifth and seventh cervical vertebrae are preserved in the holotype (PVL 4073: figures 7–9; table 3). These vertebrae are dorsoventrally low, and their centrum is oval, being transversely wider than tall. All the centra are opisthocoelous, as is usual in early tetanurans, although the anterior face is relatively flat on its centre in the anterior postaxial cervical vertebrae, resembling the condition in *Asfaltovenator vialidadi* (MPEF-PV 3440), *Condorraptor currumili* (MPEF-PV 1673–1674), *Dilophosaurus wetherilli* [23] and ceratosaurians (e.g. *Carnotaurus sastrei*: MACN-Pv CH894; *Ceratosaurus dentisulcatus* [34]; *Eoabelisaurus mefi*: MPEF-PV 3390; *Majungasaurus crenatissimus* [1]), while this face is semi-spherical in some other early tetanurans (e.g. *Allosaurus fragilis* [29]; *Eustreptospondylus oxoniensis* [40]).

In lateral view, the subcircular parapophyses emerge laterally from the anteroventral corner of the centrum. The parapophyses are more laterally projected in *Piatnitzkysaurus floresi* than in *Dilophosaurus wetherilli* [23], resembling the condition in most early averostrans (*Asfaltovenator vialidadi*: MPEF-PV 3440; *Carnotaurus sastrei*: MACN-Pv CH894; *Eoabelisaurus mefi*: MPEF-PV 3390; *Eustreptospondylus oxoniensis* [40]; *Torvosaurus tanneri* [63]). On each side of the centrum, there are two pleurocoels, one in the anterior region and the other in the posterior one, as in the anterior cervical vertebrae of *Carnotaurus sastrei* (MACN-Pv CH894), *Condorraptor currumili* (MPEF-PV 1673–1674), *Dilophosaurus wetherilli* [23], *Eoabelisaurus mefi* (MPEF-PV 3390), *Limusaurus inextricabilis* [61] and *Yunyangosaurus puanensis* [60]. In contrast, there is only one pleurocoel on each side or none in most tetanurans, such as *Allosaurus fragilis* [29] and *Sinraptor dongi* [31].

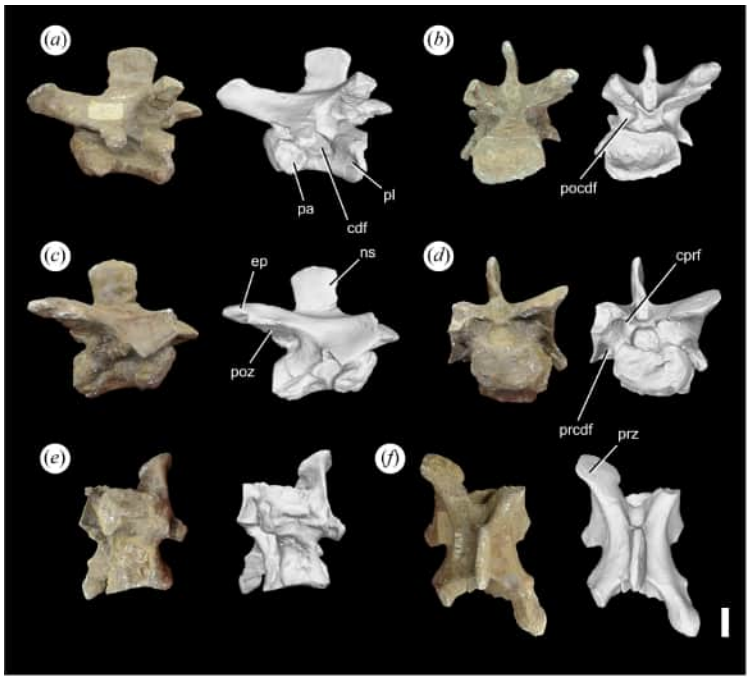

Figure 8. Photographs (left) and 3D model (right) of the fifth cervical vertebra of PVL 4073 in (*a*) left lateral, (*b*) posterior, (*c*) right lateral, (*d*) anterior, (*e*) ventral and (*f*) dorsal views. cdf, centrodiapophyseal fossa; cprf, centroprezygapophyseal fossa; ep, epipophysis; ns, neural spine; pa, parapophysis; pl, pleurocoel; pocdf, postzygapophyseal centrodiapophyseal fossa; prcdf, prezygapophyseal centrodiapophyseal fossa; poz, postzygapophysis; prz, prezygapophysis. Scale bar equals 2 cm.

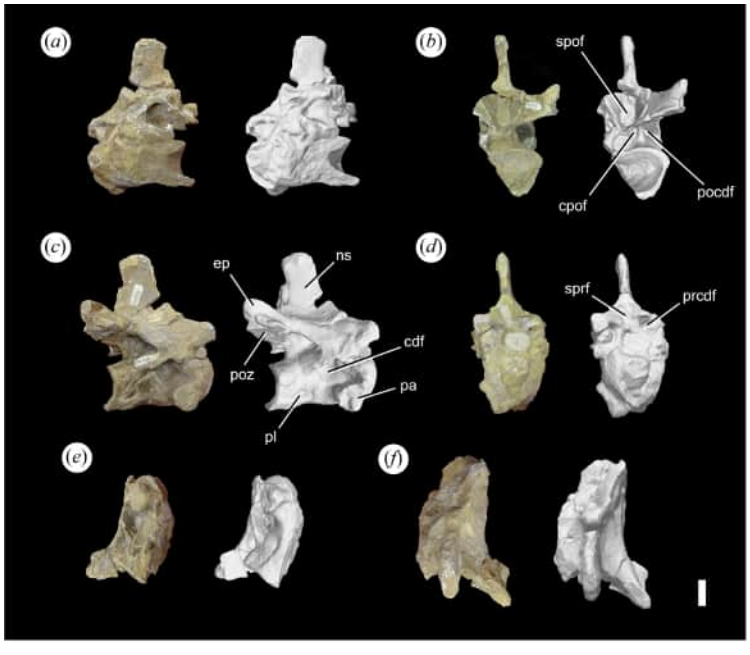

Figure 9. Photographs (left) and 3D model (right) of the seventh cervical vertebra of PVL 4073 in (*a*) left lateral, (*b*) posterior, (*c*) right lateral, (*d*) anterior, (*e*) ventral and (*f*) dorsal views. cdf, centrodiapophyseal fossa; cpof, centropostzygapophyseal fossa; ep, epipophysis; ns, neural spine; pa, parapophysis; pl, pleurocoel; pocdf, postzygapophyseal centrodiapophyseal fossa; prcdf, prezygapophyseal centrodiapophyseal fossa; poz, postzygapophysis; spof, spinopostzygapophyseal fossa; sprf, spinoprezygapophyseal fossa. Scale bar equals 2 cm.

Although this region is poorly preserved, there is no keel on the ventral surface of the anterior cervical centra, as in *Asfaltovenator vialidadi* (MPEF-PV 3440), *Eustreptospondylus oxoniensis* [40], *Limusaurus inextricabilis* [61] and *Sinraptor dongi* [31]. In contrast, *Allosaurus fragilis* [29], *Ceratosaurus dentisulcatus* [34], *Condorraptor currumili* (MPEF-PV 1673), *Dilophosaurus wetherilli* [23], *Torvosaurus*

tanneri [63] and herrerasaurids (e.g. *Herrerasaurus ischigualastensis* [54]; *Sanjuansaurus gordilloi* [55]) have a ventral keel in the anterior cervical centra. Instead of a keel, there is a shallow ventral fossa in the postaxial cervical centra in *Piatnitzkysaurus floresi* that resembles the condition in *Asfaltovenator vialidadi* (MPEF-PV 3440), the seventh centrum of *Condorraptor currumili* (MPEF-PV 1674) and the middle cervical centra of *Dilophosaurus wetherilli* [23]. In the posterior view, the edge of the posterior surface of the centrum is thickened.

The neural canal has circular anterior and posterior openings. At the base of the neural arch, there is an oval centrodiapophyseal fossa, which is relatively deep and delimited dorsally by the anterior and posterior centrodiapophyseal laminae. The diapophyses are gracile and lateroventrally oriented. In anterior view, there is a subrectangular, dorsoventrally elongated, spinoprezygapophyseal fossa just dorsal to the neural canal, which is separated from the latter by the intraprezygapophyseal lamina. This fossa is slightly dorsoventrally taller in the seventh vertebra. Laterodorsally to the neural canal, there are oval centroprezygapophyseal fossae on each side separated from the neural canal by bifurcations of the centroprezygapophyseal laminae. These fossae are shallow and smaller than the neural canal. Posterolateral to the anterior opening of the neural canal are the prezygapophyseal centrodiapophyseal fossae, separated from the canal by the centroprezygapophyseal laminae. These fossae are anteroventrally oriented and deeper than the centroprezygapophyseal fossae. In the posterior view, the neural canal is slightly more dorsoventrally compressed than in the anterior view. Dorsal to the neural canal is a subrectangular, dorsoventrally elongated, spinopostzygapophyseal fossa, which is separated from the canal by the intrapostzygapophyseal lamina. Anterolaterally to the neural canal, postzygapophyseal centrodiapophyseal fossae are separated from the canal by the centropostzygapophyseal laminae. These fossae are deeper and divided by an internal lamina in the seventh cervical vertebra. Additionally, this vertebra has two centropostzygapophyseal fossae dorsal to the neural canal. These fossae are small and shallow, separated from each other by the 'V'-shaped spinopostzygapophyseal lamina.

The prezygapophyseal facet is mainly dorsally and slightly anteromedially oriented in the fourth and fifth vertebrae. The prezygapophyseal facets are subcircular in dorsal view and more anteriorly projected than in the anterior cervical vertebrae of *Sinraptor dongi* [31], resembling the condition in most neotheropods (e.g. *Allosaurus fragilis* [29]; *Asfaltovenator vialidadi*: MPEF-PV 3440; *Dilophosaurus wetherilli* [23]; *Monolophosaurus jiangi* [56]). The epipophyses have a rounded end and are less extended in the seventh vertebra than in the anterior ones, although they are not complete. The epipophyses in *Piatnitzkysaurus floresi* are less elongated than in *Carnotaurus sastrei* (MACN-Pv CH894) and *Sinraptor dongi* [31], but more than in *Ceratosaurus dentisulcatus* [34]. Ventral to the epipophyses are the postzygapophyses, which have a subquadrangular articular facet. The neural spine is transversely narrow, and it is taller in the seventh cervical vertebra than in the fifth. The neural spine is straight and dorsally oriented, as in *Allosaurus fragilis* [29], while it is slightly posteriorly inclined in the anterior cervical vertebrae of some tetanurans (e.g. *Concavenator corcovatus* [59]; *Megalosaurus bucklandii* [37]; *Sinraptor dongi* [31]). The postaxial cervical neural spines of *Piatnitzkysaurus floresi* are taller than in *Dilophosaurus wetherilli* [23], abelisaurids (e.g. *Carnotaurus sastrei*: MACN-Pv CH894; *Majungasaurus crenatissimus* [1]) and coelophysoids (e.g. *Megapnosaurus rhodesiensis* [39]), but shorter than in *Ceratosaurus dentisulcatus* [34].

Dorsal vertebrae. Ten dorsal vertebrae are preserved in the holotype (PVL 4073: figures 10–17; tables 4 and 5), including the probable first dorsal vertebra (figure 10; although it cannot be completely ruled out that it is the last cervical vertebra). Three dorsal vertebrae are preserved in the referred specimen (MACN-Pv CH895: figures 18–20; table 5). The dorsal vertebrae comprise the tenth through the 23rd presacral vertebrae. The first dorsal centrum is opisthocoelous, while the rest are amphiplatyan to slightly amphicoelous, as is usual in early averostrans (e.g. *Allosaurus fragilis* [29]; *Carnotaurus sastrei*: MACN-Pv CH894; *Condorraptor currumili*: MPEF-PV 1676–1680, 1697, 1700, 1705; *Eustreptospondylus oxoniensis* [40]; *Monolophosaurus jiangi* [56]; *Sinraptor dongi* [31]). In contrast to the cervical vertebrae, the dorsal vertebrae are not dorsoventrally compressed. In the posterior view, the outer rim of the posterior surface of the centrum is thickened in the anterior dorsal vertebrae. The first dorsal vertebra is the only one of the dorsal series with two pleurocoels on the lateral surface of the centrum, as in the cervical vertebrae. The anterior dorsal vertebrae positioned further posteriorly bear only one anteroposteriorly elongated pleurocoel and the middle-posterior dorsal vertebrae lack pleurocoels, a similar condition to that of most non-coelurosaurian averostrans (e.g. *Allosaurus fragilis* [29]; *Condorraptor currumili*: MPEF-PV 1676–1680, 1697, 1700, 1705; *Eoabelisaurus mefi*: MPEF-PV 3390; *Limusaurus inextricabilis* [61]; *Monolophosaurus jiangi* [56]; *Yunyangosaurus puanensis* [60]), although there are some species (e.g. *Carnotaurus sastrei*: MACN-Pv CH894; *Giganotosaurus carolini*: MUCPv-CH-1; *Torvosaurus*

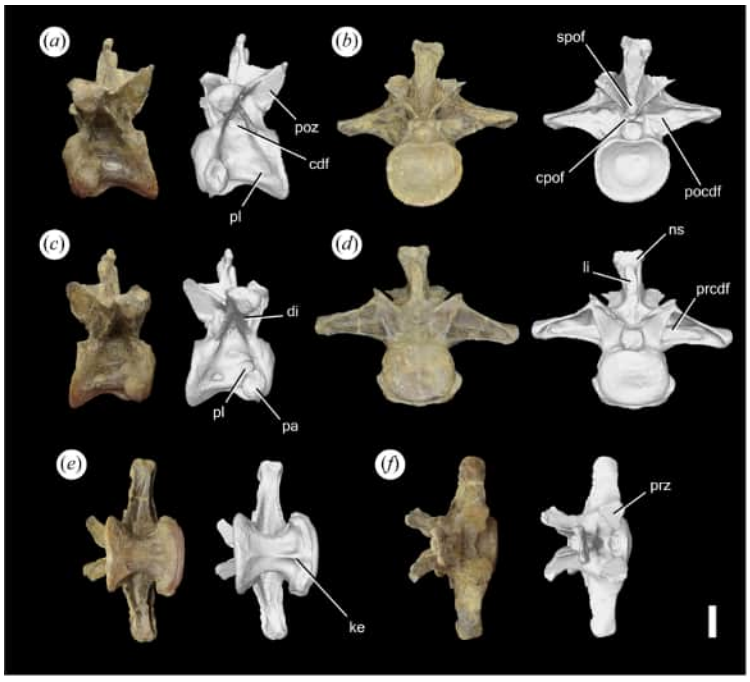

Figure 10. Photographs (left) and 3D model (right) of the tenth presacral vertebra (corresponding to the last cervical or the first dorsal vertebra) of PVL 4073 in (*a*) left lateral, (*b*) posterior, (*c*) right lateral, (*d*) anterior, (*e*) ventral and (*f*) dorsal views. cdf, centrodiapophyseal fossa; cpof, centropostzygapophyseal fossa; di, diapophysis; ke, keel; li, scar for interspinous ligament; ns, neural spine; pa, parapophysis; pl, pleurocoel; pocdf, postzygapophyseal centrodiapophyseal fossa; prcdf, prezygapophyseal centrodiapophyseal fossa; poz, postzygapophysis; prz, prezygapophysis; spof, spinopostzygapophyseal fossa. Scale bar equals 3 cm.

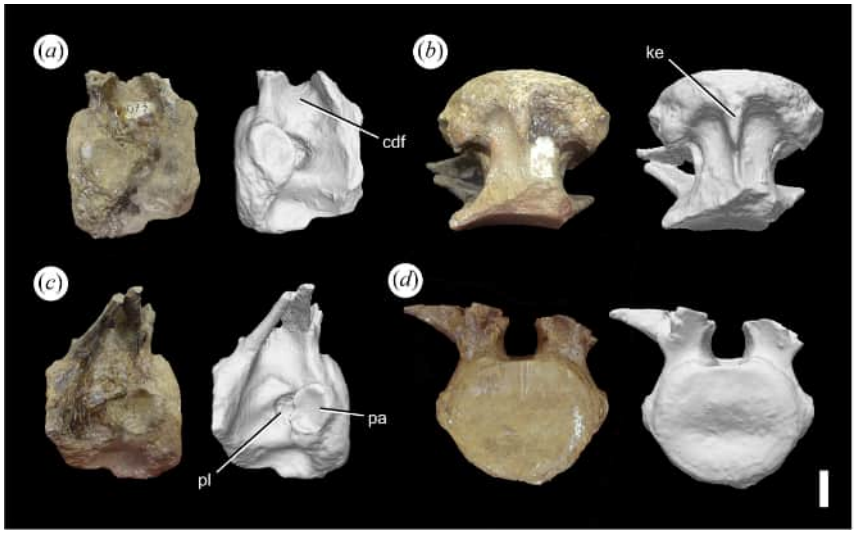

Figure 11. Photographs (left) and 3D model (right) of the eleventh presacral vertebra (corresponding to the probable second dorsal vertebra) of PVL 4073 in (*a*) left lateral, (*b*) ventral, (*c*) right lateral and (*d*) anterior views. cdf, centrodiapophyseal fossa; ke, keel; pa, parapophysis; pl, pleurocoel. Scale bar equals 2 cm.

tanneri [63]) that have pleurocoels in all or most dorsal vertebrae. A ventral keel is present only on the anterior region of the midline of the probable first three or four dorsal vertebrae, resembling the condition in *Allosaurus fragilis* [29] and *Dilophosaurus wetherilli* [23], while the keel is more posteriorly developed in *Condorraptor currumili* (MPEF-PV 1676, 1697) and *Sinraptor dongi* [31]. In contrast, a ventral keel is absent or more poorly developed in the anterior midline of the anterior dorsal vertebrae in most ceratosaurians (e.g. *Carnotaurus sastrei*: MACN-Pv CH894; *Elaphrosaurus bambergi* [64]; *Eoabelisaurus mefi*: MPEF-PV 3390; *Majungasaurus crenatissimus* [1]) and some tetanurans (e.g. *Asfaltovenator vialidadi*: MPEF-PV 3440; *Eustreptospondylus oxoniensis* [40]).

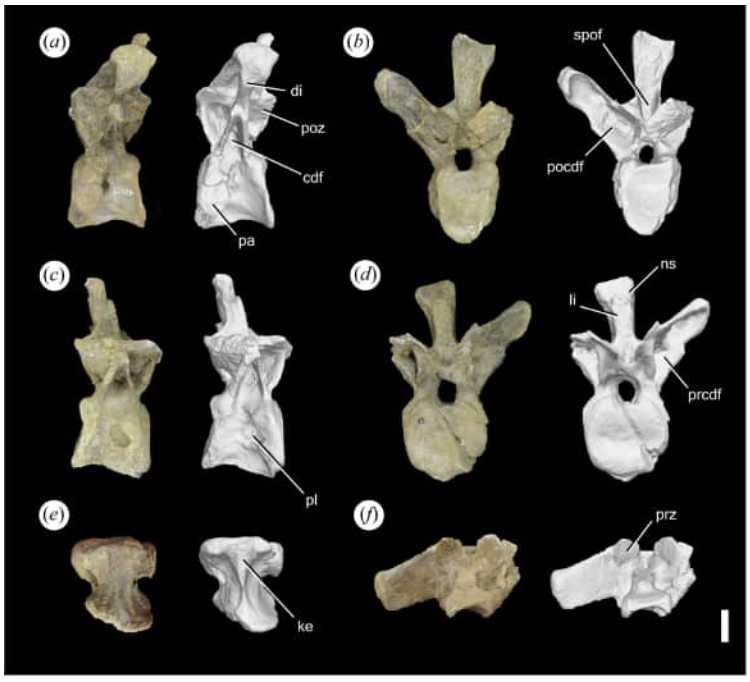

Figure 12. Photographs (left) and 3D model (right) of the thirteen presacral vertebra (corresponding to the probable fourth dorsal vertebra) of PVL 4073 in (*a*) left lateral, (*b*) posterior, (*c*) right lateral, (*d*) anterior, (*e*) ventral and (*f*) dorsal views. cdf, centrodiapophyseal fossa; di, diapophysis; ke, keel; li, scar for interspinous ligament; ns, neural spine; pa, parapophysis; pl, pleurocoel; pocdf, postzygapophyseal centrodiapophyseal fossa; prcdf, prezygapophyseal centrodiapophyseal fossa; poz, postzygapophysis; prz, prezygapophysis; spof, spinopostzygapophyseal fossa. Scale bar equals 3 cm.

The parapophyses are located anteroventrally in the anterior dorsal centra (10th and 11th presacral vertebrae) and migrate progressively into the neural arch and closer to the base of the prezygapophyses in the middle-posterior dorsal vertebrae. Posteriorly from the 17th presacral vertebra, the parapophyses are immediately ventral to the base of the prezygapophyses. In addition to changing their position, the size of the parapophyses also decreases posteriorly. In the most posterior dorsal centra, the parapophyses are on the transverse processes. The dorsal parapophyses are not projected on stalks in *Piatnitzkysaurus floresi*, in contrast to many non-tetanuran neotheropods (e.g. *Eoabelisaurus mefi*: MPEF-PV 3390; *Carnotaurus sastrei*: MACN-Pv CH894; *Ceratosaurus dentisulcatus* [34]; *Cryolophosaurus ellioti* [65]; *Majungasaurus crenatissimus* [1]). The diapophyses are gracile, laterally long and deeply excavated by fossae in all the dorsal vertebrae. The diapophyses are laterally oriented in the anterior and posterior dorsal vertebrae, while they become dorsolaterally oriented in the middle dorsal vertebrae. In contrast, the diapophyses are more posteriorly oriented in most non-coelurosaurian averostrans (e.g. *Asfaltovenator vialidadi*: MPEF-PV 3440; *Majungasaurus crenatissimus* [1]; *Monolophosaurus jiangi* [56]; *Torvosaurus tanneri* [63]) and this difference is more conspicuous in the middle-posterior dorsal vertebrae.

The prezygapophyses are positioned laterodorsal to the neural canal, and their facet is dorsomedially oriented in the first dorsal vertebra. At the same point that the parapophyses migrate in the dorsal vertebral series, the prezygapophyses become narrower, more dorsally oriented, decrease their size and change their position more medially, dorsal to the neural canal. The postzygapophyses emerge posteriorly between the neural spine and the diapophyses in the first dorsal vertebra, and their facet is lateroventrally oriented. In addition to the variations in the dorsal vertebral series, the postzygapophyses become smaller and extend less dorsolaterally in the posterior dorsal vertebrae. The hyposphene–hypantrum articulation is dorsoventrally low in the first dorsal vertebrae, although it becomes taller in the middle-posterior ones. The hyposphene is triangular in posterior view, with a dorsally facing apex, and is more posteriorly extended in the posterior dorsal vertebrae. This condition resembles that of most non-coelurosaurian neotheropods (e.g. *Allosaurus fragilis* [29]; *Asfaltovenator vialidadi*: MPEF-PV 3440; *Condorraptor currumili*: MPEF-PV 1680, 1700; *Dilophosaurus wetherilli* [23]; *Monolophosaurus jiangi* [56]; *Sinraptor dongi* [31]), although the pattern of the first appearance of this articulation in the dorsal series can differ.

Figure 13. Photographs (left) and 3D model (right) of the (*a–d*) 14th and (*e,f*) 16th presacral vertebrae (corresponding to the probable fifth and seventh dorsal vertebrae, respectively) of PVL 4073 in (*a*) left lateral, (*b,f*) right lateral, (*c*) ventral and (*d,e*) posterior views. di, diapophysis; hy, hyposphene; ns, neural spine; pa, parapophysis; pl, pleurocoel; pocdf, postzygapophyseal centrodiapophyseal fossa; spof, spinopostzygapophyseal fossa. Scale bar equals 2 cm.

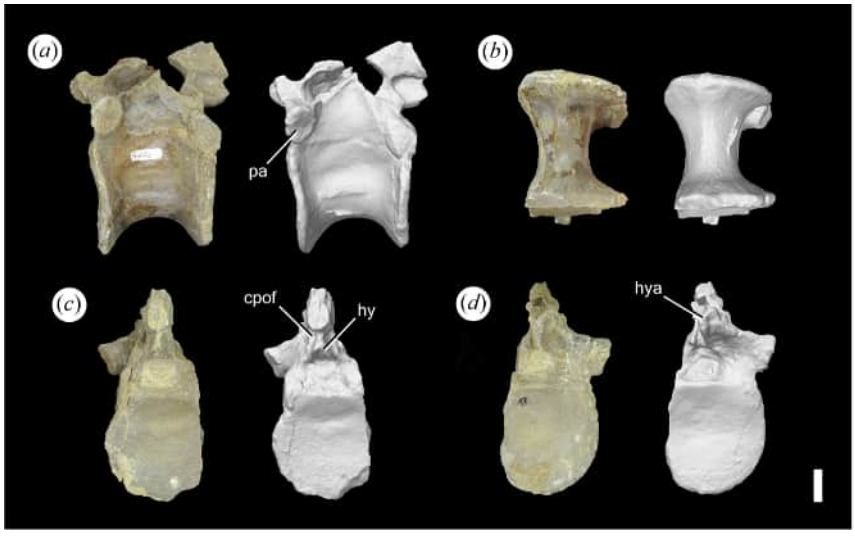

Figure 14. Photographs (left) and 3D model (right) of the seventeenth presacral vertebra (corresponding to the probable eighth dorsal vertebra) of PVL 4073 in (*a*) left lateral, (*b*) ventral, (*c*) posterior and (*d*) anterior views. cpof, centropostzygapophyseal fossa; hy, hyposphene; hya, hypantrum; pa, parapophysis. Scale bar equals 2 cm.

In anterior view, the centroprezygapophyseal fossae present in the cervical vertebrae are absent or reduced as a very shallow depression dorsolateral to the neural canal in the dorsal vertebrae, while they are well delimited and deeper in at least one dorsal vertebra in some averostrans (e.g. *Asfaltovenator vialidadi*: MPEF-PV 3440; *Carnotaurus sastrei*: MACN-Pv CH894; *Ceratosaurus dentisulcatus* [34];

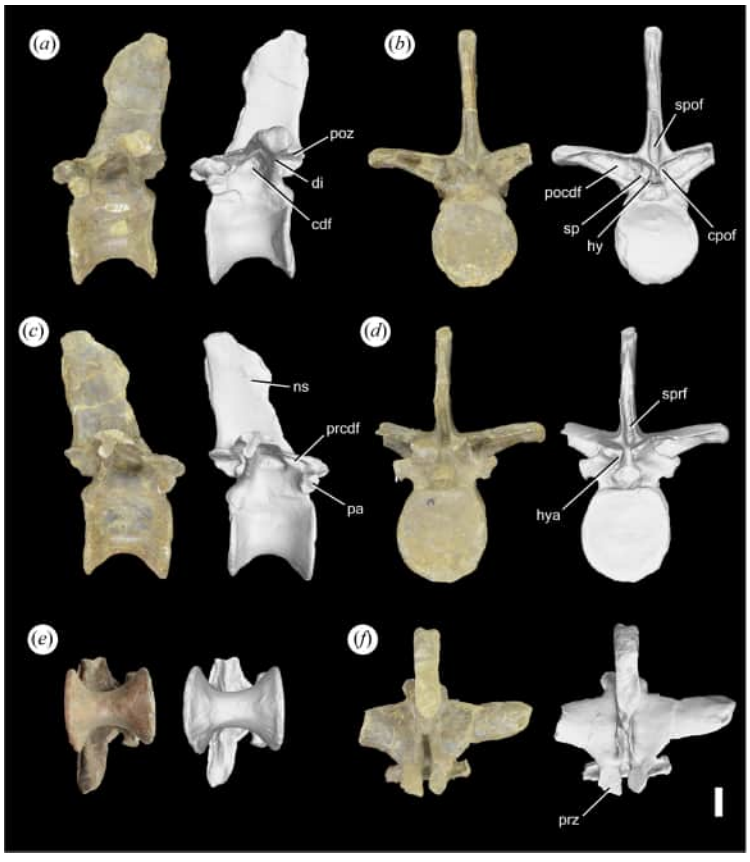

Figure 15. Photographs (left) and 3D model (right) of the 19th presacral vertebra (corresponding to the probable 10th dorsal vertebra) of PVL 4073 in (*a*) left lateral, (*b*) posterior, (*c*) right lateral, (*d*) anterior, (*e*) ventral and (*f*) dorsal views. cdf, centrodiapophyseal fossa; cpof, centropostzygapophyseal fossa; di, diapophysis; hy, hyposphene; hya, hypantrum; ns, neural spine; pa, parapophysis; pocdf, postzygapophyseal centrodiapophyseal fossa; prcdf, prezygapophyseal centrodiapophyseal fossa; poz, postzygapophysis; prz, prezygapophysis; sp, small protuberance; spof, spinopostzygapophyseal fossa; sprf, spinoprezygapophyseal fossa. Scale bar equals 3 cm.

Condorraptor currumili: MPEF-PV 1705; *Eoabelisaurus mefi*: MPEF-PV 3390; *Eustreptospondylus oxoniensis* [40]). In the anterior dorsal vertebrae, posterolateral to the neural canal, the prezygapophyseal centrodiapophyseal fossae are separated from the canal by the centroprezygapophyseal laminae. These fossae are considerably wider than in the cervical vertebrae and expand laterally onto the diapophyses and deeply medially below the prezygapophyses. In the middle-posterior dorsal vertebrae, when the parapophyses displace dorsally, the centroprezygapophyseal laminae are replaced dorsally by the prezygoparapophyseal laminae, which delimit anteriorly the prezygapophyseal centrodiapophyseal fossae. Posteriorly, these fossae are delimited by the paradiapophyseal laminae, strongly reducing the extension of the fossae on the diapophyses. These fossae are absent in the posterior dorsal vertebrae because of the fusion between the parapophyses and the diapophysis. At the height of the hypantrum, ventromedial to the prezygapophyses, there are two ventrally oriented hook-shaped projections in the middle-posterior dorsal vertebrae. These projections are also present in *Condorraptor currumili* (MPEF-PV 1705). In lateral view, at each side of the anterior dorsal vertebrae, are the centrodiapophyseal fossae that excavate the diapophyses ventrally and are delimited anteriorly and posteriorly by the anterior and posterior centrodiapophyseal laminae, respectively. In the middle-posterior dorsal vertebrae, the laminae that separate these fossae from the prezygapophyseal centrodiapophyseal fossae are the paradiapophyseal laminae, which are shorter than the anterior centrodiapophyseal laminae.

In the posterior view, anterolateral to the neural canal are the postzygapophyseal centrodiapophyseal fossae, separated from the canal by the centropostzygapophyseal laminae, as in the cervical vertebrae. These fossae are extended laterally along the diapophyses. The postzygapophyseal centrodiapophyseal fossae are separated from the anterior centrodiapophyseal fossae by the posterior centrodiapophyseal laminae. The first dorsal vertebra has two centropostzygapophyseal fossae

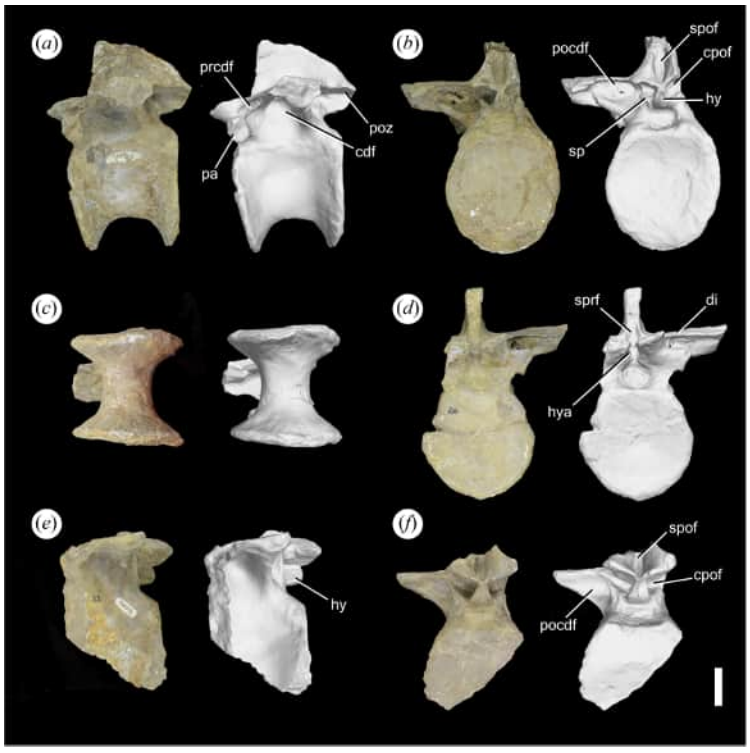

Figure 16. Photographs (left) and 3D model (right) of the (*a–d*) 20th and (*e,f*) 22nd presacral vertebrae (corresponding to the probable 11th and 13th dorsal vertebrae, respectively) of PVL 4073 in (*a,e*) left lateral, (*b,f*) posterior, (*c*) ventral and (*d*) anterior views. cdf, centrodiapophyseal fossa; cpof, centropostzygapophyseal fossa; di, diapophysis; hy, hyposphene; hya, hypantrum; pa, parapophysis; pocdf, postzygapophyseal centrodiapophyseal fossa; prcdf, prezygapophyseal centrodiapophyseal fossa; poz, postzygapophysis; sp, small protuberance; spof, spinopostzygapophyseal fossa; sprf, spinoprezygapophyseal fossa. Scale bar equals 3 cm.

dorsal to the neural canal, as in the seventh cervical vertebra. These fossae are small and shallow, separated from each other by the V-shaped spinopostzygapophyseal lamina. The centropostzygapophyseal fossae are positioned laterally on both sides of the hyposphene in the middle-posterior dorsal vertebrae. These fossae are partially connected to the postzygapophyseal centrodiapophyseal fossae, but there are two small, dorsolaterally oriented protuberances over the centropostzygapophyseal laminae between both fossae in the middle-posterior dorsal vertebrae. These protuberances are only present in *Piatnitzkysaurus floresi* and *Condorraptor currumili* and are positioned at each side, ventrolateral to the hyposphene. In *Marshosaurus bicentesimus* (CMNH 21704), there are prominent ridges that separate both fossae instead of protuberances. The anterior dorsal vertebrae have slight thickenings instead of protuberances at the same position.

The anterior dorsal vertebrae have transversely wide neural spines, which are transversely more robust than in the cervical vertebrae. Posterior to the probable thirteenth presacral (third dorsal) vertebra, the neural spines become anteroposteriorly deeper, transversely narrower and taller. Scars of interspinous ligament attachments are present on the anterior and posterior surfaces of the neural spines of the tenth (last cervical or first dorsal) and the thirteenth (third dorsal) presacral vertebrae, as in the anteriormost dorsal vertebrae of *Allosaurus fragilis* [29]. The dorsal neural spines of *Piatnitzkysaurus floresi* are proportionally taller than in *Carnotaurus sastrei* (MACN-Pv CH894) and shorter than in *Ceratosaurus dentisulcatus* [34], *Eoabelisaurus mefi* (MPEF-PV 3390) and *Sinraptor dongi* [31], resembling the height of *Asfaltovenator vialidadi* (MPEF-PV 3440), *Allosaurus fragilis* [29], *Monolophosaurus jiangi* [56] and *Torvosaurus tanneri* [63]. In the anterior view, there is a subrectangular, dorsoventrally elongated spinoprezygapophyseal fossa dorsal to the neural canal, and both structures are separated from each other by the intraprezygapophyseal lamina, as in the cervical vertebrae. This lamina is reduced in the posterior dorsal vertebrae. The spinoprezygapophyseal fossa is reduced in the anterior dorsal vertebrae and is gently dorsally extended over the neural spine in the middle dorsal vertebrae. In the posterior view, dorsal to the neural canal, separated by the intrapostzygapophyseal lamina and the hyposphene, there is the subrectangular spinopostzygapophyseal fossa, which is reduced in the

Figure 17. Photographs (left) and 3D model (right) of the last dorsal vertebra (corresponding to the probable 14th dorsal vertebra) articulated with the first 4th sacral vertebrae of PVL 4073 in (*a*) left lateral, (*b*) right lateral, (*c*) ventral, (*d*) dorsal, (*e*) posterior and (*f*) anterior views. hya, hypantrum; ns, neural spine; prz, prezygapophysis; sr, sacral rib; tp, transverse process. Scale bar equals 5 cm.

anterior dorsal vertebrae and extends dorsally slightly onto the neural spine in the middle dorsal vertebrae.

Sacrum. Four sacral vertebrae (1st to 4th) are preserved in the holotype (PVL 4073: figure 17), while five sacral vertebrae (1st to 5th) are preserved in the referred specimen (MACN-Pv CH895: figures 21 and 22; table 6), indicating that the sacrum was composed of five vertebrae. This is the usual number of sacral vertebrae in neotheropods (e.g. *Alpkarakush kyrgyzicus* [66]; *Coelophysis bauri* [44]; *Concavenator corcovatus* [59]; *Eustreptospondylus oxoniensis* [40]; *Megalosaurus bucklandii* [37]; *Meraxes gigas* [9]; *Sinraptor dongi* [31]; *Tyrannosaurus rex* [67]), although ceratosaurs usually have more sacral vertebrae (e.g. *Carnotaurus sastrei*: MACN-Pv CH894; *Elaphrosaurus bambergi* [64]; *Eoabelisaurus mefi*: MPEF-PV 3390; *Masiakasaurus knopfleri* [36]; *Vespersaurus paranaensis* [68]). Non-neotheropod saurischians have less than five sacral vertebrae (e.g. *Eodromaeous murphi* [69]; *Herrerasaurus ischigualastensis*: PVL 2566). In the holotype of *Piatnitzkysaurus floresi*, the sacral centra are fused from the first to the fourth element and preserved articulated with the last dorsal vertebra. The zygapophyses are also fused between each other in the 2nd to 4th sacral elements of the holotype. In the referred specimen, the sacral vertebrae are fused from the second to the fourth element and preserved articulated to the last sacral vertebra, while the first sacral vertebra is preserved disarticulated. This difference in the number of fused sacral vertebrae could indicate that the holotype specimen would be a skeletally more mature specimen. In contrast, none of the fused sacral vertebrae are present in *Eustreptospondylus oxoniensis* [40] and *Sinraptor dongi* [31]. Suture lines are absent between the fused centra, as in *Condorraptor currumili* (MPEF-PV 1681) and *Megalosaurus bucklandii* [37].

The sacral vertebrae of *Piatnitzkysaurus floresi* are amphiplatyan. The vertebral centra of the first and fifth sacral vertebrae are anteroposteriorly shorter than in the middle sacral elements, as in some tetanuran theropods (e.g. *Eustreptospondylus oxoniensis* [40]; *Meraxes gigas* [9]; *Tyrannotitan chubutensis* [8]), but contrasting with the subequal or shorter anteroposterior length of the middle sacral vertebrae of some other tetanurans and non-tetanuran neotheropods (e.g. *Alpkarakush kyrgyzicus* [66]; *Carnotaurus sastrei*: MACN-Pv CH894; *Ceratosaurus nasicornis* [33]; *Coelophysis bauri* [44]; *Concavenator corcovatus*

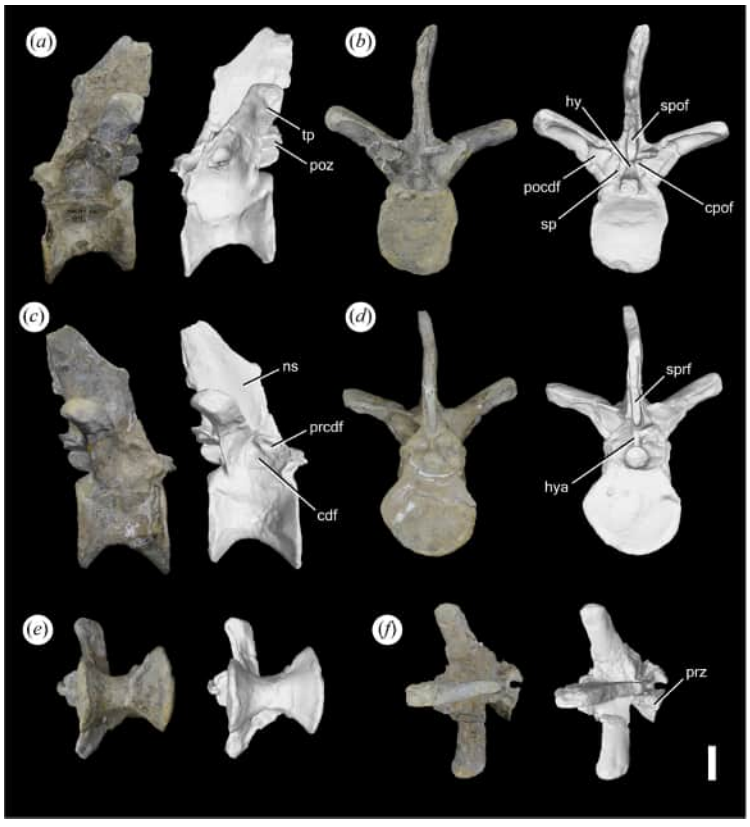

Figure 18. Photographs (left) and a 3D model (right) of a mid-posterior dorsal vertebra of MACN-Pv CH895 in (*a*) left lateral, (*b*) posterior, (*c*) right lateral, (*d*) anterior, (*e*) ventral and (*f*) dorsal views. cdf, centrodiapophyseal fossa; cpof, centropostzygapophyseal fossa; hy, hyposphene; hya, hypantrum; ns, neural spine; pocdf, postzygapophyseal centrodiapophyseal fossa; prcdf, prezygapophyseal centrodiapophyseal fossa; poz, postzygapophysis; prz, prezygapophysis; sp, small protuberance; spof, spinopostzygapophyseal fossa; sprf, spinoprezygapophyseal fossa; tp, transverse process. Scale bar equals 3 cm.

[59]; *Megalosaurus bucklandii* [37]; *Pendraig milnerae* [70]). In the first sacral vertebra of *Piatnitzkysaurus floresi*, the anterior edge of the vertebral centrum thickens and extends ventrally more than the posterior edge, while between the 2nd and 4th sacral vertebrae these edges are similarly extended ventrally. In the fifth sacral vertebra, the posterior edge of the vertebral centrum is more ventrally extended than the anterior edge. This extension of the anterior and posterior edges in the first and last sacral vertebrae, respectively, is a usual condition in neotheropods (e.g. *Allosaurus fragilis* [29]; *Carnotaurus sastrei*: MACN-Pv CH894; *Condorraptor currumili*: MPEF-PV 1701; *Dilophosaurus wetherilli* [23]; *Eustreptospondylus oxoniensis* [40]; *Meraxes gigas* [9]; *Tyrannosaurus rex* [67]). The extension and thickening of the anteroventral margin of the first sacral centrum is more developed than in other early neotheropods (e.g. *Allosaurus fragilis* [29]; *Condorraptor currumili*: MPEF-PV 1701; *Dilophosaurus wetherilli* [23]; *Eoabelisaurus mefi*: MPEF-PV 3390; *Eustreptospondylus oxoniensis* [40]; *Megalosaurus bucklandii* [37]). The first and fifth sacral centra are the transversely widest, while the middle sacral elements are slightly compressed both transversely and dorsoventrally, although not as much as in non-tetanuran neotheropods (e.g. *Carnotaurus sastrei*: MACN-Pv CH894; *Ceratosaurus nasicornis* [34]; *Coelophysis bauri* [44]; *Majungasaurus crenatissimus* [1]; *Pendraig milnerae* [70]). The posterodorsal margin of the vertebral centrum of the first sacral vertebra extends dorsolaterally, partially surrounding the neural canal, as in *Condorraptor currumili* (MPEF-PV 1701) and *Eustreptospondylus oxoniensis* [40], although it is less pronounced in the latter.

Two intervertebral foramina that perforate the sacrum are present in the referred specimen between the second and the fourth sacral vertebrae. These foramina are also present in the holotype and in *Condorraptor currumili* (MPEF-PV 1681), but they are covered by matrix. These foramina resemble the condition in *Megalosaurus bucklandii* [37]. No pleurocoels are present, as in ceratosaurians and some early tetanurans (e.g. *Aucasaurus garridoi* [71]; *Carnotaurus sastrei*: MACN-Pv CH894; *Condorraptor currumili*: MPEF-PV 1681, 1701; *Vespersaurus paranaensis* [69]; *Sinraptor dongi* [31]), in contrast to carcharodontosaurids and some coelurosaurians (e.g. *Giganotosaurus carolini*: MUCPv-CH-1; *Mapusaurus roseae* [6]; *Tyrannotitan chubutensis* [8]; megaraptorans, tyrannosaurids [72]). Numerous nutrient

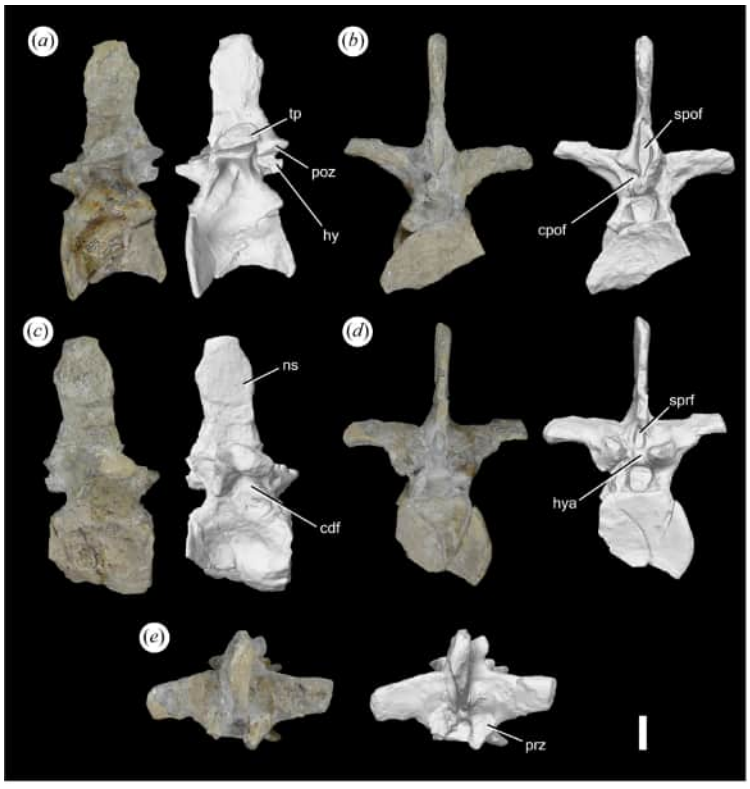

Figure 19. Photographs (left) and 3D model (right) of a posterior dorsal vertebra of MACN-Pv CH895 in (*a*) left lateral, (*b*) posterior, (*c*) right lateral, (*d*) anterior and (*e*) dorsal views. cdf, centrodiapophyseal fossa; cpof, centropostzygapophyseal fossa; hy, hyposphene; hya, hypantrum; ns, neural spine; poz, postzygapophysis; prz, prezygapophysis; spof, spinopostzygapophyseal fossa; sprf, spinoprezygapophyseal fossa; tp, transverse process. Scale bar equals 3 cm.

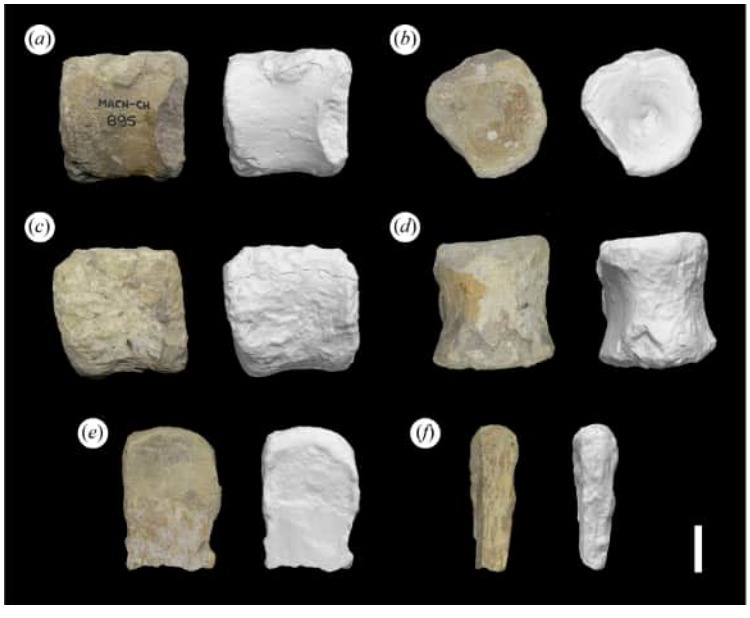

Figure 20. Photographs (left) and 3D model (right) of (*a–d*) a dorsal vertebral centrum and (*e,f*) a neural spine of MACN-Pv CH895 in (*a*) left lateral, (*b,f*) posterior, (*c,e*) right lateral and (*d*) ventral views. Scale bar equals 3 cm.

foramina are present on both lateral sides of the first sacral vertebral centrum. There are no keels present on the ventral surface of the sacral vertebrae, in contrast to *Alpkarakush kyrgyzicus* [66], *Cryolophosaurus ellioti* [65] and *Megalosaurus bucklandii* [37], which have a keel in at least one sacral vertebra; the ventral surface is rather flat to rounded in all the sacral vertebrae of *Piatnitzkysaurus*

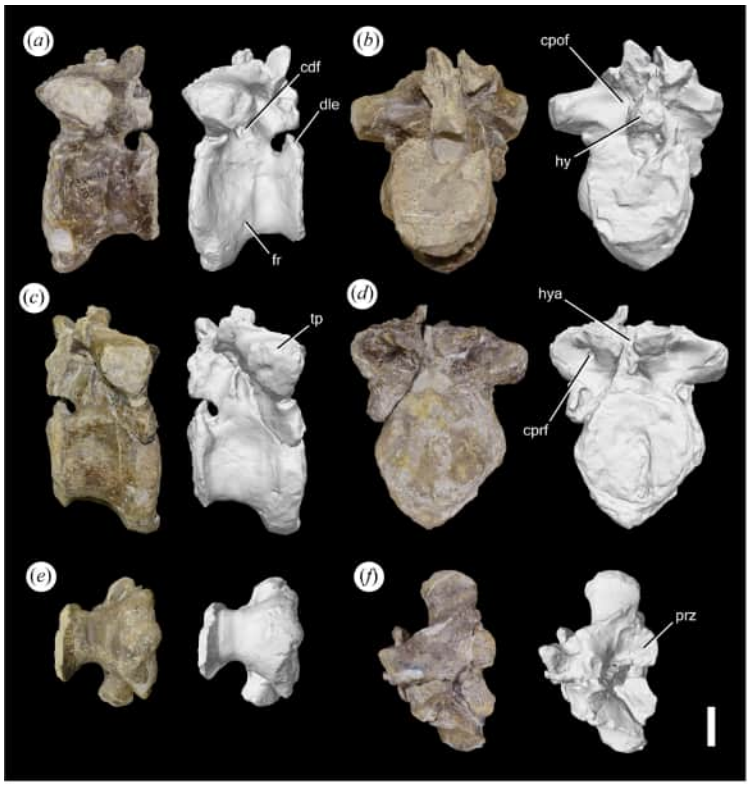

Figure 21. Photographs (left) and 3D model (right) of first sacral vertebra of MACN-Pv CH895 in (*a*) left lateral, (*b*) posterior, (*c*) right lateral, (*d*) anterior, (*e*) ventral and (*f*) dorsal views. cdf, centrodiapophyseal fossa; cpof, centropostzygapophyseal fossa; cprf, centroprezygapophyseal fossa; dle, dorsolateral extension; fr, foramen; hy, hyposphene; hya, hypantrum; prz, prezygapophyses; tp, transverse process. Scale bar equals 3 cm.

floresi. The ventral margin of the sacrum bows dorsally in lateral view, as is usual in non-coelurosaurian averostrans (e.g. *Alpkarakush kyrgyzicus* [66]; *Aucasaurus garridoi* [71]; *Carnotaurus sastrei*: MACN-Pv CH894; *Concavenator corcovatus* [59]; *Elaphrosaurus bambergi* [64]; *Giganotosaurus carolini*: MUCPv-CH-1; *Megalosaurus bucklandii* [37]).

The transverse processes are laterally oriented anteriorly, becoming laterodorsally oriented towards the posterior end of the sacrum. In lateral view, the transverse processes are dorsoventrally elongated, as in *Allosaurus fragilis* [29], but the first sacral transverse process is circular, as in *Alpkarakush kyrgyzicus* [66] and *Sinraptor dongi* [31]. The articular facet for the sacral ribs and the transverse processes is distinct from each other in the first four sacral vertebrae. The holotype is more complete, and there is an advanced degree of fusion between these articular surfaces and the sacral ribs, especially in the third and fourth sacral elements. The transverse process is anteriorly positioned in the first three sacral vertebrae, while it is more posteriorly positioned in the last two sacral vertebrae. The prezygapophyses and postzygapophyses between the 2nd and 4th sacral vertebrae are fused between each other or poorly preserved in the case of the second sacral element. The prezygapophyses in the first sacral vertebra are wider laterally than in the last dorsal vertebra. The postzygapophyses in the first sacral vertebra are more dorsally extended than in the last dorsal vertebra. The postzygapophyses in the fifth sacral vertebra are similar to those of the last dorsal vertebra, although in the fifth sacral element, they are more dorsally extended. The hyposphene in the first sacral vertebra is wider laterally and more robust than in the last dorsal vertebra, and the hyposphene in the last sacral vertebra resembles the condition in the last dorsal vertebra. A low, robust ridge running across the base of the transverse process, from the posterolateral corner of the prezygapophysis to the anterolateral corner of the postzygapophysis, is present at both lateral sides of the first sacral vertebra, as in *Condorraptor currumili* (MPEF-PV 1701).

In anterior view, the circular centroprezygapophyseal fossae are present just ventral to the anterolaterally oriented prezygapophyses in the first sacral vertebra. The morphology of these fossae resembles those in *Condorraptor currumili* (MPEF-PV 1701), while they are larger in *Eustreptospondylus oxoniensis* [40] and absent in several other early tetanurans (e.g. *Allosaurus fragilis* [29]; *Megalosaurus bucklandii* [37]). In lateral view, there are centrodiapophyseal fossae at the mid-dorsal height on each

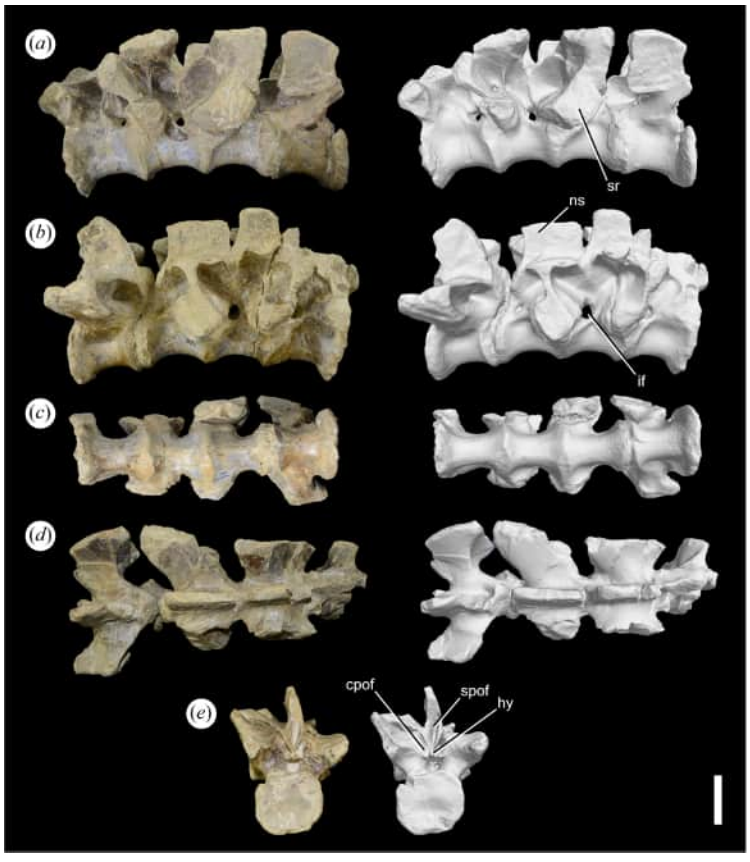

Figure 22. Photographs (left) and 3D model (right) of the second to fifth sacral vertebrae of MACN-Pv CH895 in (*a*) left lateral, (*b*) right lateral, (*c*) ventral, (*d*) dorsal and (*e*) posterior views. cpof, centropostzygapophyseal fossa; hy, hyposphene; if, intervertebral foramen; ns, neural spine; spof, spinopostzygapophyseal fossa; sr, sacral rib. Scale bar equals 5 cm.

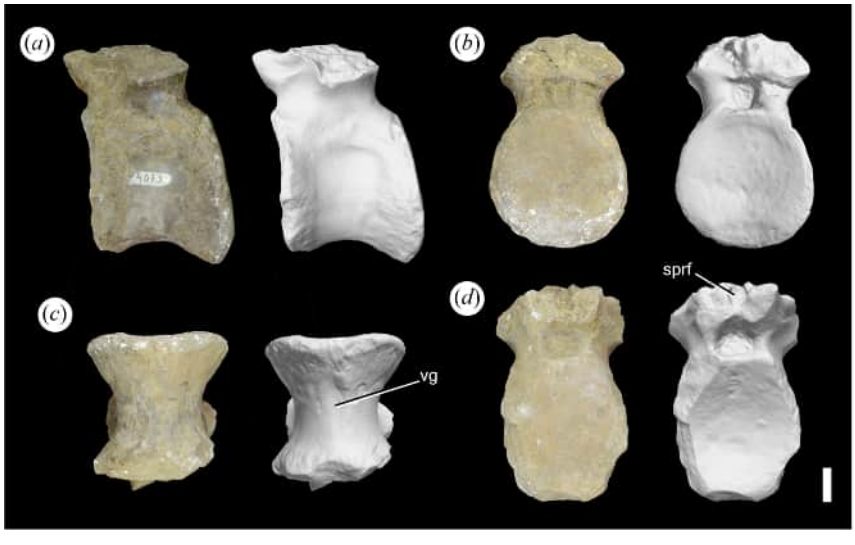

Figure 23. Photographs (left) and 3D model (right) of an anterior caudal vertebra of PVL 4073 in (*a*) left lateral, (*b*) posterior, (*c*) ventral and (*d*) anterior view. sprf, spinoprezygapophyseal fossa; vg, ventral groove. Scale bar equals 2 cm.

side of the first sacral vertebral centrum, which extend dorsally to excavate the ventral surface of the transverse processes. The centropostzygophyseal fossae occur posterodorsal to each of these fossae and are separated from the centrodiapophyseal fossae by the centrodiapophyseal laminae. In the posterior view, the centropostzygapophyseal fossae are located lateral to both sides of the hyposphene in the fifth sacral vertebra, as in *Alpkarakush kyrgyzicus* [66] and *Sinraptor dongi* [31], and resembling the condition in the posterior dorsal vertebrae of *Piatnitzkysaurus floresi*.

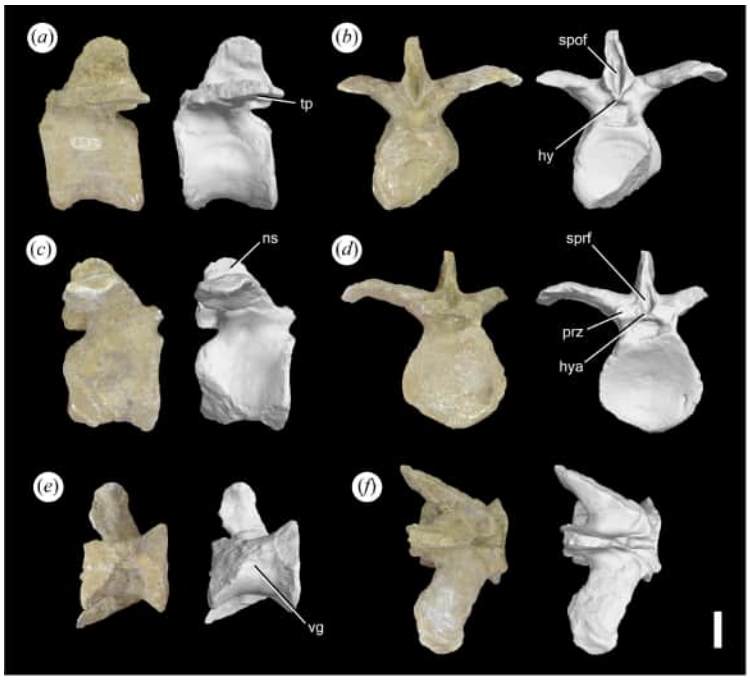

Figure 24. Photographs (left) and 3D model (right) of an anterior caudal vertebra of PVL 4073 in (*a*) left lateral, (*b*) posterior, (*c*) right lateral, (*d*) anterior, (*e*) ventral and (*f*) dorsal views. hy, hyposphene; hya, hypantrum; ns, neural spine; prz, prezygapophysis; spof, spinopostzygapophyseal fossa; sprf, spinoprezygapophyseal fossa; tp, transverse process; vg, ventral groove. Scale bar equals 3 cm.

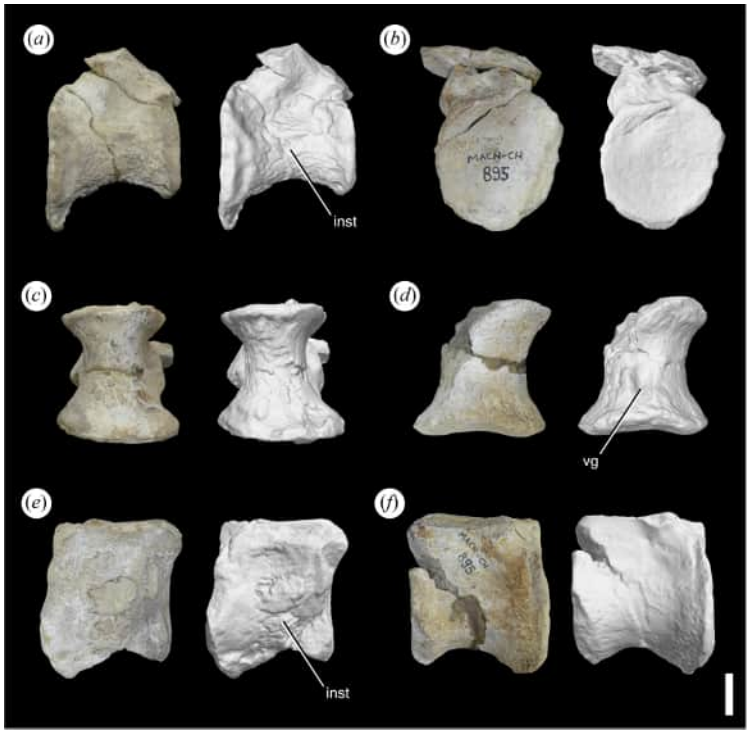

Figure 25. Photographs (left) and 3D model (right) of two anterior caudal centra (*a–c* and *d–f*, respectively) of MACN-Pv CH895 in (*a,f*) left lateral, (*b*) anterior, (*c,d*) ventral and (*e*) right lateral views. inst, internal structure; vg, ventral groove. Scale bar equal to 3 cm.

The neural spines are mainly dorsally oriented and slightly posterior. Although they are incomplete, there are no signs of fusion between the sacral neural spines, as in most allosauroids (e.g. *Allosaurus fragilis* [29]; *Giganotosaurus carolini*: MUCPv-CH-1; *Tyrannotitan chubutensis* [8]), in contrast to the condition in most ceratosaurians and some tetanurans (e.g. *Aucasaurus garridoi* [71]; *Carnotaurus*

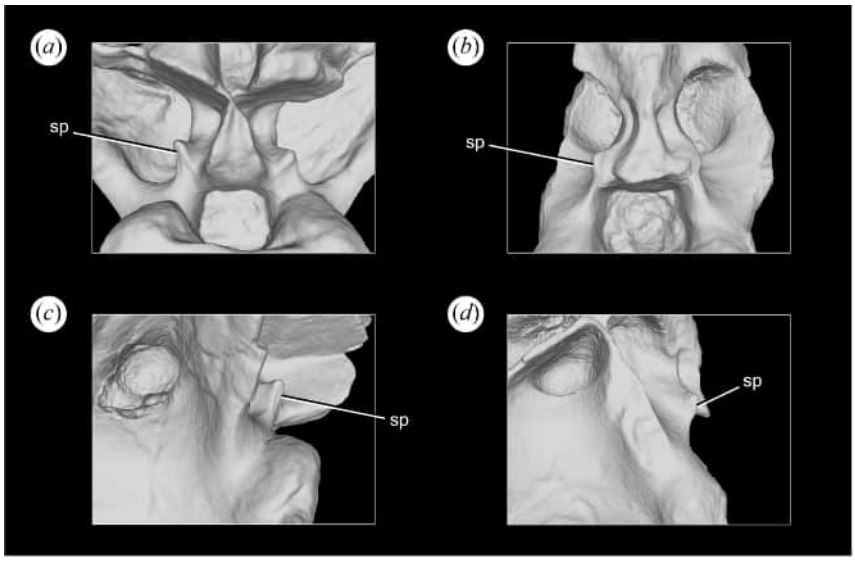

Figure 26. 3D model of (*a,c*) a middle-posterior dorsal vertebra of *Piatnitzkysaurus floresi* (MACN-Pv CH895) and (*b,d*) a middle-posterior dorsal vertebra of *Condorraptor currumili* (MPEF-PV 1705) in (*a,b*) posterior and (*c,d*) lateral views. sp, small protuberance.

sastrei: MACN-Pv CH894; *Elaphrosaurus bambergi* [64]; *Eoabelisaurus mefi*: MPEF-PV 3390; *Masiakasaurus knopfleri* [36]; *Megalosaurus bucklandii* [37]; *Meraxes gigas* [9]; *Tyrannosaurus rex* [67]).

Caudal vertebrae—Two anterior caudal vertebrae are preserved in the holotype (PVL 4073: figures 23, 24; table 6) and two anterior caudal vertebral centra are preserved in the referred specimen (MACN-Pv CH895: figure 25). The presence of a median longitudinal groove on the ventral surface and the size of the vertebrae allow them to be identified as anterior caudal vertebrae. In general, all the caudal vertebrae of *Piatnitzkysaurus floresi* are poorly preserved. All the centra are slightly amphicoelous or amphiplatyan, as is usual in theropods (e.g. *Allosaurus fragilis* [29]; *Carnotaurus sastrei*: MACN-Pv CH894; *Cryolophosaurus ellioti* [65]; *Dilophosaurus wetherilli* [23]; *Eustreptospondylus oxoniensis* [40]; *Tyrannotitan chubutensis* [8]), in contrast to some coelurosaurians, which have some opisthocoelus anterior caudal vertebrae (e.g. *Dineobellator notohesperus*, *Gigantoraptor erlianensis* [73]). The shape of the centra resembles the last sacral centra. The anterior margin of the vertebral centrum in one of the caudal vertebrae of the referred specimen is notoriously more ventrally expanded than the posterior margin, in contrast to *Ceratosaurus nasicornis* [33], *Condorraptor currumili* (MPEF-PV 1682–1683, 1702) and some megalosauroids (*Eustreptospondylus oxoniensis* [40]; *Megalosaurus bucklandii* [37]; *Monolophosaurus jiangi* [56]), in which the posterior margin is more ventrally expanded. The margins in the other caudal centra of *Piatnitzkysaurus* are similarly expanded, as in *Allosaurus fragilis* [29] and *Sinraptor dongi* [31].

The centra have a median longitudinal groove on the ventral surface, which posteriorly reaches the facet for the haemal arch. This groove, surrounded laterally by low keels, is usually present in at least one anterior caudal vertebra of most theropods (e.g. *Allosaurus fragilis* [29]; *Ceratosaurus nasicornis* [33]; *Dilophosaurus wetherilli* [23]; *Eustreptospondylus oxoniensis* [40]; *Megalosaurus bucklandii* [37]; *Monolophosaurus jiangi* [56]), although in some others many of the anterior caudal vertebrae have a rounded ventral surface without grooves (e.g. *Condorraptor currumili*: MPEF-PV 1683, 1702; *Cryolophosaurus ellioti* [65]; *Eoabelisaurus mefi*: MPEF-PV 3390). There is no evidence of pneumatization in the centrum and neural arches of the caudal vertebrae of *Piatnitzkysaurus floresi*.

In the only caudal vertebra that preserves the transverse processes, they are posterolaterally oriented in dorsal view and slightly dorsally oriented in anterior view. The most complete of these transverse processes has a conspicuous ventral bowing, but it is probably a result of post-mortem deformation. The hyposphene and the postzygapophyses are similar to those of the last sacral vertebra. The anterior caudal vertebrae have shallow centrodiapophyseal fossae below the transverse processes and shallow centropostzygapophyseal fossae located laterally at both sides of the hyposphene. The centropostzygapophyseal fossae are deeper in *Condorraptor currumili* (MPEF-PV 1682–1683, 1702). The spinoprezygapophyseal fossa, anteriorly and the spinopostzygapophyseal fossa, posteriorly, are dorsoventrally expanded above the neural canal.

5. Discussion

5.1. Tooth replacement in *Piatnitzkysaurus floresi*

A mesiodistal sequence of alternate maturity of teeth along the tooth row (i.e. Zahnreihe [74]) can be identified in the dentary and at least up to the 11th alveolus in the maxilla, where a more matured tooth is preceded by a younger one. Odd and even teeth have similar maturity developments, respectively. This same condition is present in recent works about the dentition in tyrannosaurids [75–77]. Although studies of dental replacement patterns in Theropoda are remarkably scarce, the presence of a similar pattern in tyrannosauroids and the Early Jurassic *Piatnitzkysaurus* suggests this pattern may represent the generalized condition of, at least, Tetanurae. More broadly, a similar pattern is also present in the sauropodomorph *Europasaurus holgeri* [78] and the dinosaur precursor *Lewisuchus admixtus* [79], which in turn suggest a possible common pattern since the origins of Dinosauromorpha.

In dorsal view, the smallest replacement teeth are close to the lingual margin, as in other theropods [75,76]. As it was previously mentioned, there are some cases in the maxilla and dentary of teeth that are erupting while there are still roots that have not been fully absorbed in the same alveolus. This situation, combined with the development of the emerging teeth in the position of the pulp cavity of the older tooth [75,80], can be clearly observed in tooth positions 2nd and 7th of the dentary (figure 5). The presence of three teeth in different stages of maturation in the same alveolus has also been observed in previous works focused on theropods [75]. In the most immature teeth, the cusp can be differentiated, in accordance with previous works that analysed that the cusp is one of the first regions that develops during dental ontogeny [75,81]. There is no simultaneous development of the mesial and distal teeth in the maxilla, as it occurs in *Tarbosaurus bataar* [75]. This pattern cannot be observed in the dentary of *Piatnitzkysaurus floresi* because it is incomplete.

5.2. Diagnostic features and number of individuals of *Piatnitzkysaurus floresi*

An emended diagnosis for *Piatnitzkysaurus floresi* is presented in this study. A maxilla with the base of the ascending process strongly medially inflated, exceeding the rest of the inner surface of the bone, is a character state modified from the diagnosis proposed by Rauhut [42]. We agree with the recognition of this feature as autapomorphic for *Piatnitzkysaurus floresi*, but it should be noted that the maxilla is unknown in *Condorraptor currumili*. The widening at the base of the ascending process of the maxilla houses a large pneumatic cavity enclosed by very thin bony walls, as shown by the micro-CT scan (figure 4*b*,*c*). This cavity corresponds to the promaxillary sinus, which is posteriorly connected to the maxillary antrum, forming the maxillary sinus [82]. The promaxillary sinus of *Piatnitzkysaurus floresi* is particularly anterolaterally expanded, more than in other non-avian neotheropods [82–84] and living birds [84–86]. Further studies on early tetanurans are required to clarify whether this feature represents a condition widespread among non-coelurosaurian tetanurans or a unique trait of *Piatnitzkysaurus floresi*.

It is impossible to know the degree of expansion of the maxillary sinus in *Piatnitzkysaurus floresi* because of the partial preservation of both maxillae, although it is not extended posteroventrally in the maxilla, in contrast to the coelurosaurian *Alioramus*. In this latter species, the maxillary sinus appears to penetrate the alveoli close to the root of the teeth, but it could be an artefact of the CT scan segmentation [82]. Previous studies have related this maxillary cavity with the nasal cavity and suggested it could have had functions associated with ventilation or physiology, involving air sacs, although there are still few studies on the possible function of these pneumatic sinuses in non-avian theropods [82–84,87–89]. In the maxilla of *Piatnitzkysaurus floresi*, we interpret canals and foramina in the middle-posterior region of the bone as part of the neurovascular system. The premaxilla is unknown in *Piatnitzkysaurus floresi*, so it is impossible to determine any potential extensions of the promaxillary sinus into this bone.

The maxillary fenestra has a straight, longitudinally oriented ventral margin in both preserved maxillae of *Piatnitzkysaurus floresi* (figure 4*a*). The segmented 3D model of the referred maxilla (figure 3) shows that the remains of the ascending process were probably wrongly glued because its ventral margin is not continuous with the dorsal margin in the rest of the bone. Thus, in the reconstruction of the complete maxilla (figure 4*a*), we infer that the angle between the ascending and the horizontal processes of the maxilla would be smaller, since the detached fragment probably belonged to a more

dorsal section. Based on this reconstruction and the anterior end of the frontal ventrally flexed, the rostrum of *Piatnitzkysaurus floresi* would have been dorsoventrally lower and anteroposteriorly longer than previously inferred [20], resembling the condition in *Dilophosaurus wetherilli* [23] and *Marshosaurus bicentesimus* [35], rather than that of allosauroids (e.g. *Allosaurus fragilis* [29]; *Sinraptor dongi* [31]) and *Asfaltovenator vialidadi* [16]. However, in *Dilophosaurus wetherilli* and *Marshosaurus bicentesimus* [35], the anteromedial process is positioned ventrally (just above the interdental plates), contrasting with the more dorsal position in *Piatnitzkysaurus floresi*. Additionally, the anteroventral margin of the maxilla curves dorsally in *Dilophosaurus wetherilli* [23], while this margin is straight in *Piatnitzkysaurus floresi*. This combination of character states in the maxilla of *Piatnitzkysaurus floresi* is unique and distinguishes this taxon from other early neotheropods.

Among the diagnostic features of the postcranium, the mid-posterior dorsal vertebrae of *Piatnitzkysaurus floresi* have two ventrally oriented, hook-shaped projections located at the level of the hypantrum, ventromedial to the prezygapophyses. These vertebrae also have pointed protuberances positioned lateral to the centropostzygapophyseal laminae. These projections at the anterior face and protuberances at the posterior face of the mid-posterior vertebrae are also present in *Condorraptor currumili*, although the protuberances are rounded/bulbous instead of pointed in the latter species (figure 26). However, there are few well-preserved vertebrae of *Condorraptor currumili*, and some posterior dorsal vertebrae are unknown in *Piatnitzkysaurus floresi*, so this variation could be a product of serial variation in the dorsal vertebrae. The contact between these structures occurs in the sagittal plane, the anterior projections wedging between the hyposphene and the posterior protuberances. They may have reinforced the intervertebral joint anteroposteriorly and restricted the lateral movements of the trunk. These projections and protuberances are a unique character state of *Piatnitzkysaurus* and *Condorraptor* in Theropoda.

In the first sacral vertebra of *Piatnitzkysaurus floresi*, the anteroventral edge of the vertebral centrum thickens and extends ventrally. This condition is present in the referred specimen and is absent in *Condorraptor currumili*, while the first sacral vertebra is ventrally broken in the holotype. The ilium has a vertical ridge at the level of the base of the ischiatic peduncle, which is also present in *Monolophosaurus jiangi*. A similar condition is present in *Megalosaurus bucklandii*, although its ridge is considerably shorter [37, fig. 14]. The distal tarsal 4 of *Piatnitzkysaurus floresi* is notably broad transversely at its posterior end, more than in other neotheropods (e.g. *Allosaurus fragilis* [29]; *Powellvenator podocitus* [90]; *Sinraptor dongi* [31]).

This series of autapomorphies or unique combination of character states supports the taxonomic validity of *Piatnitzysaurus floresi*. Also, the few and minor anatomical differences between the holotype and referred specimen endorse the referral of the latter to *Pianitzkysaurus floresi*. These two specimens were found in a bone bed together with multiple sauropod specimens [14], and Bonaparte [20] identified the presence of two individuals in the original description of these materials. Pradelli *et al* [22] found two left ilia among the remains catalogued under MACN-Pv CH895, which could indicate the presence of a third individual. In the PVL collection, we could only identify a partial postacetabular process of a right ilium [22]. Bonaparte [20, p. 9] only listed 'fragments of ilium' for the holotype and did not mention any ilium for the referred specimen. Some pages later, Bonaparte [20, p. 33] provided some measurements for the ilium of the holotype of *Piatnitzkysaurus floresi,* and based on them it seems that the most complete ilium could be that of the holotype, but it currently lacks any collection number on it. Thus, it is likely that the iliac bones were mixed between the MACN and PVL collections, and one of the left ilia at the MACN collection is actually from the holotype. In conclusion, we do not find conclusive evidence to support that there are more than two individuals in the hypodigm of *Piatnitzkysaurus floresi*.

Ethics. This work did not require ethical approval from a human subject or animal welfare committee.

Data accessibility. Three-dimensional models of axial and skull bones of both PVL 4073 and MACN-Pv CH895 made by photogrammetry, and the three-dimensional renderings of the right maxilla of MACN-Pv CH 895 and the left dentary of PVL 4073 (including the raw z-slices) made from the micro-CT scan, are available in MorphoSource at https://www.morphosource.org/projects/000758836.

Declaration of AI use. We have not used AI-assisted technologies in creating this article.

Authors' contributions. L.A.P.: conceptualization, data curation, formal analysis, investigation, methodology, validation, visualization, writing—original draft, writing—review and editing; D.P.: conceptualization, investigation, methodology, supervision, validation, writing—review and editing; N.A.V.: conceptualization, investigation, methodology, validation, writing—review and editing; M.D.E.: conceptualization, investigation, methodology, supervision, validation, writing—review and editing.

All authors gave final approval for publication and agreed to be held accountable for the work performed therein.

Conflict of interest declaration. We declare we have no competing interests.

Funding. This research was supported by the Agencia Nacional de Promoción Científica y Técnica (PICT 2018-01186 to M.D.E. and PICT 2019-03834 to D.P.).

Acknowledgements. We thank Pablo Ortiz and Rodrigo González (PVL) for allowing access to the PVL collection in order to study the holotype of *Piatnitzkysaurus floresi*. We are grateful to Eduardo Ruigómez (MPEF-PV) for allowing access to the MPEF-PV collection and facilitating the study of *Condorraptor currumili*. We want to thank Belén von Baczko for helping in the segmentation of the micro-CT scan and Agustín Martinelli for comments on the interpretation of the tooth roots in the micro-CT scan. We greatly appreciate the comments and suggestions of two anonymous reviewers, which improved the quality of this manuscript.

References

1. O'Connor PM. 2007 The postcranial axial skeleton of *Majungasaurus crenatissimus* (Theropoda: Abelisauridae) from the late cretaceous of Madagascar. *J. Vertebr. Paleontol*. **27**, 127–163. (doi:10.1671/0272-4634(2007)27[127:tpasom]2.0.co;2)
2. Rolando AMA, Motta MJ, Agnolín FL, Tsuihiji T, Miner S, Brissón-Egli F, Novas FE. 2024 A new carcharodontosaurid specimen sheds light on the anatomy of South American giant predatory dinosaurs. *Sci. Nat*. **111**, 56. (doi:10.1007/s00114-024-01942-4)
3. Osborn HF. 1905 Tyrannosaurus and other Cretaceous carnivorous dinosaurs. In *Proc. Acad. Natural Sciences of Philadelphia*, vol. **8**, p. 72, American Museum of Natural History (New York).
4. Gauthier J. 1986 Saurischian monophyly and the origin of birds. *Memoirs Calif. Acad. Sci*. **8**, 1–55.
5. Coria RA, Salgado L. 1995 A new giant carnivorous dinosaur from the cretaceous of Patagonia. *Nature* **377**, 224–226. (doi:10.1038/377224a0)
6. Coria RA, Currie PJ. 2006 A new carcharodontosaurid (Dinosauria, Theropoda) from the upper cretaceous of Argentina. *Geodiversitas* **28**, 71–118.
7. Xu X, Wang K, Zhang K, Ma Q, Xing L, Sullivan C, Hu D, Cheng S, Wang S. 2012 A gigantic feathered dinosaur from the lower cretaceous of China. *Nature* **484**, 92–95. (doi:10.1038/nature10906)
8. Canale JI, Novas FE, Pol D. 2015 Osteology and phylogenetic relationships of *Tyrannotitan chubutensis* Novas, de Valais, Vickers-Rich and Rich, 2005 (Theropoda: Carcharodontosauridae) from the Lower Cretaceous of Patagonia, Argentina. *Hist. Biol*. **27**, 1–32. (doi:10.1080/08912963.2013.861830)
9. Canale JI *et al*. 2022 New giant carnivorous dinosaur reveals convergent evolutionary trends in theropod arm reduction. *Curr. Biol*. **32**, 3195–3202.(doi:10.1016/j.cub.2022.05.057)
10. Prum RO, Berv JS, Dornburg A, Field DJ, Townsend JP, Lemmon EM, Lemmon AR. 2015 A comprehensive phylogeny of birds (Aves) using targeted next-generation DNA sequencing. *Nature* **526**, 569–573. (doi:10.1038/nature15697)
11. Allain R, Tykoski R, Aquesbi N, Jalil NE, Monbaron M, Russell D, Taquet P. 2007 An abelisauroid (Dinosauria: Theropoda) from the Early Jurassic of the High Atlas Mountains, Morocco, and the radiation of ceratosaurs. *J. Vertebr. Paleontol*. **27**, 610–624. (doi:10.1671/0272-4634(2007)27[610:aadtft]2.0.co;2)
12. Dal Sasso C, Maganuco S, Cau A. 2018 The oldest ceratosaurian (Dinosauria: Theropoda), from the Lower Jurassic of Italy, sheds light on the evolution of the three-fingered hand of birds. *PeerJ* **6**, e5976. (doi:10.7717/peerj.5976)
13. Pol D, Rauhut OWM. 2012 A Middle Jurassic abelisaurid from Patagonia and the early diversification of theropod dinosaurs. *Proc. R. Soc. B Biol. Sci*. **279**, 3170–3175. (doi:10.1098/rspb.2012.0660)
14. Bonaparte JF. 1979 Dinosaurs: a jurassic assemblage from patagonia. *Science* **205**, 1377–1379. (doi:10.1126/science.205.4413.1377)
15. Rauhut OWM. 2005 Osteology and relationships of a new theropod dinosaur from the Middle Jurassic of Patagonia. *Palaeontology* **48**, 87–110. (doi:10.1111/j.1475-4983.2004.00436.x)
16. Rauhut OWM, Pol D. 2019 Probable basal allosauroid from the early Middle Jurassic Cañadón Asfalto Formation of Argentina highlights phylogenetic uncertainty in tetanuran theropod dinosaurs. *Sci. Rep*. **9**, 18826. (doi:10.1038/s41598-019-53672-7)
17. Cúneo R, Ramezani J, Scasso R, Pol D, Escapa I, Zavattieri AM, Bowring SA. 2013 High-precision U–Pb geochronology and a new chronostratigraphy for the Cañadón Asfalto Basin, Chubut, central Patagonia: Implications for terrestrial faunal and floral evolution in Jurassic. *Gondwana Res*. **24**, 1267–1275. (doi:10.1016/j.gr.2013.01.010)
18. Figari EG, Scasso RA, Cúneo RN, Escapa I. 2015 Estratigrafía y evolución geológica de la Cuenca de Cañadón Asfalto, Provincia del Chubut, Argentina. *Lat. Am. J. Sedimentol. Basin Anal*. **22**, 135–169.
19. Pol D, Ramezani J, Gomez K, Carballido JL, Carabajal AP, Rauhut OWM, Escapa IH, Cúneo NR. 2020 Extinction of herbivorous dinosaurs linked to Early Jurassic global warming event. *Proc. R. Soc. B* **287**, 20202310. (doi:10.1098/rspb.2020.2310)
20. Bonaparte JF. 1986 The dinosaurs (carnosaurs, allosaurids, sauropods, cetiosaurids) of the Middle Jurassic of Cerro Cóndor (Chubut, Argentina. *Ann. De Paléontol* **72**, 325–386.
21. Rauhut OWM. 2004 Braincase structure of the Middle Jurassic theropod dinosaur *Piatnitzkysaurus*. *Can. J. Earth Sci*. **41**, 1109–1122. (doi:10.1139/e04-053)
22. Pradelli LA, Pol D, Ezcurra MD. 2024 The appendicular osteology of the Early Jurassic theropod *Piatnitzkysaurus floresi* and its implications on the morphological disparity of non-coelurosaurian tetanurans. *Zool. J. Linn. Soc*. **203**, zlae176. (doi:10.1093/zoolinnean/zlae176)

23. Marsh AD, Rowe TB. 2020 A comprehensive anatomical and phylogenetic evaluation of *Dilophosaurus wetherilli* (Dinosauria, Theropoda) with descriptions of new specimens from the Kayenta Formation of northern Arizona. *J. Paleontol*. **94**, 1–103. (doi:10.1017/jpa.2020.14)
24. Pradelli LA, Pol D, Ezcurra MD. 2024 New dinosaur remains increase theropod diversity in the Cañadón Asfalto formation (Lower Jurassic), Chubut Province, Argentina. *J. Syst. Palaeontol*. **22**, 2318262. (doi:10.1080/14772019.2024.2318262)
25. Owen R. 1842 Report on British fossil reptiles. *Rep. Br. Assoc. Adv. Sci*. **11**, 60–204.
26. Padian K, May CL. 1993 The earliest dinosaurs. *N. M. Mus. Nat. Hist. Sci. Bull*. **3**, 379–381.
27. Marsh OC. 1881 Principal characters of American Jurassic dinosaurs, Part V. *Am. J. Sci*. **s3-21**, 417–423. (doi:10.2475/ajs.s3-21.125.417)
28. Holtz TR, Molnar RE, Currie PJ. 2004 Basal Tetanurae. In *The Dinosauria* (eds DB Weishampel, P Dodson, H Osmolska), pp. 71–110, 2nd edn. Berkeley, CA: University of California Press. (doi:10.1525/california/9780520242098.003.0006)
29. Madsen JH. 1976 Allosaurus fragilis: a revised osteology. *Utah Geol. Miner. Surv. Bull*. **109**, 1–163.
30. Sampson SD, Witmer LM. 2007 Craniofacial anatomy of *Majungasaurus crenatissimus* (Theropoda: Abelisauridae) from the Late Cretaceous of Madagascar. *J. Vertebr. Paleontol*. **27**, 32–104. (doi:10.1671/0272-4634(2007)27[32:caomct]2.0.co;2)
31. Currie PJ, Zhao XJ. 1993 A new carnosaur (Dinosauria, Theropoda) from the Jurassic of Xinjiang, People's Republic of China. *Can. J. Earth Sci*. **30**, 2037–2081. (doi:10.1139/e93-179)
32. Paulina-Carabajal A, Filippi L. 2018 Neuroanatomy of the abelisaurid theropod Viavenator : the most complete reconstruction of a cranial endocast and inner ear for a South American representative of the clade. *Cretac. Res*. **83**, 84–94. (doi:10.1016/j.cretres.2017.06.013)
33. Gilmore CW. 1920 *Osteology of the carnivorous Dinosauria in the United States National Museum: with special reference to the genera Antrodemus (Allosaurus) and Ceratosaurus*. Washington, DC: US Government Printing Office. (doi:10.5479/%20si.03629236.110.i)
34. Madsen JH, Welles SP. 2000 *Ceratosaurus (dinosauria, theropoda): a revised osteology*, pp. 1–80. Salt Lake City, UT: Utah Geological Survey Miscellaneous Publication.
35. Madsen JH. 1976 A second new theropod dinosaur from the Late Jurassic of East Central Utah. *Utah Geol*. **3**, 51–60. (doi:10.34191/ug-3-1_51)
36. Carrano MT, Sampson SD, Forster CA. 2002 The osteology of *Masiakasaurus knopfleri* , a small abelisauroid (Dinosauria: Theropoda) from the Late Cretaceous of Madagascar. *J. Vertebr. Paleontol*. **22**, 510–534. (doi:10.1671/0272-4634(2002)022[0510:toomka]2.0.co;2)
37. Benson RBJ. 2010 A description of *Megalosaurus bucklandii* (Dinosauria: Theropoda) from the Bathonian of the UK and the relationships of Middle Jurassic theropods. *Zool. J. Linn. Soc*. **158**, 882–935. (doi:10.1111/j.1096-3642.2009.00569.x)
38. Hendrickx C, Mateus O. 2014 *Torvosaurus gurneyi* n. sp., the largest terrestrial predator from Europe, and a proposed terminology of the maxilla anatomy in nonavian theropods. *PLoS ONE* **9**, e88905. (doi:10.1371/journal.pone.0088905)
39. Raath MA. 1977 The anatomy of the Triassic theropod *Syntarsus rhodesiensis* (Saurischia: Podokesauridae) and a consideration of its biology. PhD thesis, Rhodes University, Grahamstown, South Africa.
40. Sadleir R, Barrett PM, Powell HP. 2006 The anatomy and systematics of *Eustreptospondylus oxoniensis* , a theropod dinosaur from the Middle Jurassic of Oxfordshire, England. *Monogr. Palaeontogr. Soc*. **160**, 1–82. (doi:10.1080/25761900.2022.12131807)
41. Brusatte SL, Benson RBJ, Currie PJ, Xijin Z. 2010 The skull of *Monolophosaurus jiangi* (Dinosauria: Theropoda) and its implications for early theropod phylogeny and evolution. *Zool. J. Linn. Soc*. **158**, 573–607. (doi:10.1111/j.1096-3642.2009.00563.x)
42. Rauhut OWM. 2003 The interrelationships and evolution of basal theropod dinosaurs. *Special Papers in Palaeontology* **69**, 1–213.
43. Eddy DR, Clarke JA. 2011 New information on the cranial anatomy of *Acrocanthosaurus atokensis* and its implications for the phylogeny of Allosauroidea (Dinosauria: Theropoda). *PLoS One* **6**, e17932. (doi:10.1371/journal.pone.0017932)
44. Rinehart LF, Lucas SG, Heckert AB, Spielmann JA, Celeskey MD. 2009 *The paleobiology of Coelophysis bauri (Cope) from the Upper Triassic (Apachean) Whitaker Quarry, New Mexico, with detailed analysis of a single quarry block*. Albuquerque, NM: New Mexico Museum of Natural History.
45. You HL, Azuma Y, Wang T, Wang YM, Dong ZM. 2014 The first well-preserved coelophysoid theropod dinosaur from Asia. *Zootaxa* **3873**, 233–249. (doi:10.11646/zootaxa.3873.3.3)
46. Zhao XJ, Currie PJ. 1993 A large crested theropod from the Jurassic of Xinjiang, People's Republic of China. *Can. J. Earth Sci*. **30**, 2027–2036. (doi:10.1139/e93-178)
47. Hendrickx C, Mateus O, Araujo R. 2015 The dentition of megalosaurid theropods. *Acta Palaeontol. Pol*. **60**, 627–642. (doi:10.4202/app.00056.2013)
48. Meso JG, Hendrickx C, Baiano MA, Canale JI, Salgado L, Diaz Martinez I. 2021 Isolated theropod teeth associated with a sauropod skeleton from the allen formation (Campanian–maastrichtian, Upper Cretaceous) of Río Negro, Patagonia, Argentina. *Acta Palaeontol. Pol*. **66**, 409–423. (doi:10.4202/app.00847.2020)
49. Zaher H, Pol D, Navarro BA, Delcourt R, Carvalho AB. 2020 An Early Cretaceous theropod dinosaur from Brazil sheds light on the cranial evolution of the Abelisauridae. *Comptes Rendus Palevol* **19**, 101–115. (doi:10.5852/cr-palevol2020v19a6)
50. Hendrickx C, Mateus O, Lourinhã M, Araújo R, Lourinhã M, Choiniere J. 2019 The distribution of dental features in non-avian theropod dinosaurs: taxonomic potential, degree of homoplasy, and major evolutionary trends. *Palaeontol. Electron*. **22**, 74. (doi:10.26879/820)
51. Rauhut OWM. 2004 Provenance and anatomy of *Genyodectes serus* , a large-toothed ceratosaur (Dinosauria: Theropoda) from Patagonia. *J. Vertebr. Paleontol*. **24**, 894–902. (doi:10.1671/0272-4634(2004)024[0894:paaogs]2.0.co;2)
52. Wilson JA. 1999 A nomenclature for vertebral laminae in sauropods and other saurischian dinosaurs. *J. Vertebr. Paleontol*. **19**, 639–653. (doi:10.1080/02724634.1999.10011178)
53. Wilson JA, D'Emic MD, Ikejiri T, Moacdieh EM, Whitlock JA. 2011 A nomenclature for vertebral fossae in sauropods and other saurischian dinosaurs. *PLoS One* **6**, e17114. (doi:10.1371/journal.pone.0017114)

54. Sereno PC, Novas FE. 1994 The skull and neck of the basal theropod *Herrerasaurus ischigualastensis*. *J. Vertebr. Paleontol*. **13**, 451–476. (doi:10.1080/02724634.1994.10011525)
55. Alcober OA, Martínez RN. 2010 A new herrerasaurid (Dinosauria, Saurischia) from the Upper Triassic Ischigualasto Formation of northwestern Argentina. *Zookeys* **63**, 55–81. (doi:10.3897/zookeys.63.550)
56. Xi-jin Z, Benson RBJ, Brusatte SL, Currie PJ. 2010 The postcranial skeleton of *Monolophosaurus jiangi* (Dinosauria: Theropoda) from the Middle Jurassic of Xinjiang, China, and a review of Middle Jurassic Chinese theropods. *Geol. Mag*. **147**, 13–27. (doi:10.1017/s0016756809990240)
57. Pacheco C, Müller RT, Langer M, Pretto FA, Kerber L, Dias da Silva S. 2019 *Gnathovorax cabreirai*: a new early dinosaur and the origin and initial radiation of predatory dinosaurs. *PeerJ* **7**, e7963. (doi:10.7717/peerj.7963)
58. Pol D, Garrido A, Cerda IA. 2011 A new sauropodomorph dinosaur from the Early Jurassic of Patagonia and the origin and evolution of the sauropod-type sacrum. *PLoS One* **6**, e14572. (doi:10.1371/journal.pone.0014572)
59. Cuesta E, Ortega F, Sanz JL. 2019 Axial osteology of *Concavenator corcovatus* (Theropoda; Carcharodontosauria) from the Lower Cretaceous of Spain. *Cretac. Res*. **95**, 106–120. (doi:10.1016/j.cretres.2018.10.026)
60. Dai H *et al*. 2020 A new possible megalosauroid theropod from the Middle Jurassic Xintiangou Formation of Chongqing, People's Republic of China and its implication for early tetanuran evolution. *Sci. Rep*. **10**, 139. (doi:10.1038/s41598-019-56959-x)
61. Stiegler JB. 2019 *Anatomy, systematics, and paleobiology of noasaurid ceratosaurs from the Late Jurassic of China*. Washington, DC: George Washington University.
62. Gao Y. 1992 *Yangchuanosaurus hepingensis* – a new species of carnosaur from Zigong, Sichuan. *Vertebr. Palasiat*. **30**, 313–324.
63. Britt BB. 1991 Theropods of Dry Mesa Quarry (Morrison Formation, late Jurassic), Colorado, with emphasis on the osteology of Torvosaurus tanneri. *Brigh. Young Univ. Geol. Stud*. **37**, 1–72.
64. Rauhut OWM, Carrano MT. 2016 The theropod dinosaur *Elaphrosaurus bambergi* Janensch, 1920, from the Late Jurassic of Tendaguru, Tanzania. *Zool. J. Linn. Soc*. **178**, 546–610. (doi:10.1111/zoj.12425)
65. Smith ND, Makovicky PJ, Hammer WR, Currie PJ. 2007 Osteology of *Cryolophosaurus ellioti* (Dinosauria: Theropoda) from the Early Jurassic of Antarctica and implications for early theropod evolution. *Zool. J. Linn. Soc*. **151**, 377–421. (doi:10.1111/j.1096-3642.2007.00325.x)
66. Rauhut OWM, Bakirov AA, Wings O, Fernandes AE, Hübner TR. 2024 A new theropod dinosaur from the Callovian Balabansai Formation of Kyrgyzstan. *Zool. J. Linn. Soc*. **201**, zlae090. (doi:10.1093/zoolinnean/zlae090)
67. Brochu CA. 2003 Osteology of *Tyrannosaurus rex*: insights from a nearly complete skeleton and high-resolution computed tomographic analysis of the skull. *J. Vertebr. Paleontol*. **22**, 1–138. (doi:10.2307/3889334)
68. Langer MC *et al*. 2019 A new desert-dwelling dinosaur (Theropoda, Noasaurinae) from the Cretaceous of south Brazil. *Sci. Rep*. **9**, 9379. (doi:10.1038/s41598-019-45306-9)
69. Martinez RN, Sereno PC, Alcober OA, Colombi CE, Renne PR, Montañez IP, Currie BS. 2011 A basal dinosaur from the dawn of the dinosaur era in southwestern Pangaea. *Science* **331**, 206–210. (doi:10.1126/science.1198467)
70. Spiekman SNF, Ezcurra MD, Butler RJ, Fraser NC, Maidment SCR. 2021 *Pendraig milnerae* , a new small-sized coelophysoid theropod from the Late Triassic of Wales. *R. Soc. Open Sci*. **8**, 210915. (doi:10.1098/rsos.210915)
71. Baiano MA, Coria R, Chiappe LM, Zurriaguz V, Coria L. 2023 Osteology of the axial skeleton of *Aucasaurus garridoi*: phylogenetic and paleobiological inferences. *PeerJ* **11**, e16236. (doi:10.7717/peerj.16236)
72. Rolando AMA, Brissón-Egli F, Sales MA, Martinelli AG, Canale JI, Ezcurra MD. 2018 A supposed Gondwanan oviraptorosaur from the Albian of Brazil represents the oldest South American megaraptoran. *Cretac. Res*. **84**, 107–119. (doi:10.1016/j.cretres.2017.10.019)
73. Jasinski SE, Sullivan RM, Carter AM, Johnson EH, Dalman SG, Zariwala J, Currie PJ. 2023 Osteology and reassessment of *Dineobellator notohesperus*, a southern eudromaeosaur (Theropoda: Dromaeosauridae: Eudromaeosauria) from the latest Cretaceous of New Mexico. *Anat. Rec*. **306**, 1712–1756. (doi:10.1002/ar.25103)
74. DeMar R. 1972 Evolutionary implications of Zahnreihen. *Evolution* **26**, 435–450. (doi:10.1111/j.1558-5646.1972.tb01948.x)
75. Hanai T, Tsuihiji T. 2019 Description of tooth ontogeny and replacement patterns in a juvenile *Tarbosaurus bataar* (Dinosauria: Theropoda) using CT-scan data. *Anat. Rec*. **302**, 1210–1225. (doi:10.1002/ar.24014)
76. Sattler F, Schwarz D. 2021 Tooth replacement in a specimen of *Tyrannosaurus rex* (Dinosauria, Theropoda) from the Hell Creek Formation (Maastrichtian), Montana. *Hist. Biol*. **33**, 949–972. (doi:10.1080/08912963.2019.1675052)
77. Ke YH, Pei R, Xu X. 2024 High-resolution CT-scan data reveals the tooth replacement pattern of the Late Jurassic tyrannosauroid *Guanlong wucaii* (Dinosauria, Theropoda). *Vertebr. Palasiat* **62**, 225–244. (doi:10.19615/j.cnki.2096-9899.240715)
78. Régent V, Wiersma-Weyand K, Wings O, Knötschke N, Sander PM. 2024 The dentition of the Late Jurassic dwarf sauropod *Europasaurus holgeri* from northern Germany: ontogeny, function, and implications for a rhamphotheca-like structure in Sauropoda. *PeerJ* **12**, e17764. (doi:10.7717/peerj.17764)
79. Ezcurra MD, Nesbitt SJ, Fiorelli LE, Desojo JB. 2020 New specimen sheds light on the anatomy and taxonomy of the early Late Triassic dinosauriforms from the Chañares Formation, NW Argentina. *Anat. Rec*. **303**, 1393–1438. (doi:10.1002/ar.24243)
80. Edmund AG. 1969 Dentition. In *Biology of the Reptilia, vol. 1: morphology* (eds C Gans, AA Bellairs, TS Parsons), pp. 115–200. London, UK: Academic Press.
81. Romer AS, Parsons TS. 1977 *The vertebrate body*, 5th edn. Philadelphia, PA: WB Saunders Company.
82. Gold MEL, Brusatte SL, Norell MA. 2013 The cranial pneumatic sinuses of the Tyrannosaurid *Alioramus* (Dinosauria: Theropoda) and the evolution of cranial pneumaticity in theropod dinosaurs. *Am. Mus. Novit*. **2013**, 1–46. (doi:10.1206/3790.1)

83. Tahara R, Larsson HCE. 2011 Cranial pneumatic anatomy of *Ornithomimus edmontonicus* (Ornithomimidae: Theropoda). *J. Vertebr. Paleontol*. **31**, 127–143. (doi:10.1080/02724634.2011.539646)
84. Brownstein CD. 2021 Dromaeosaurid crania demonstrate the progressive loss of facial pneumaticity in coelurosaurian dinosaurs. *Zool. J. Linn. Soc*. **191**, 87–112. (doi:10.1093/zoolinnean/zlaa048)
85. Witmer LM. 1990 The craniofacial air sac system of Mesozoic birds (Aves). *Zool. J. Linn. Soc*. **100**, 327–378. (doi:10.1111/j.1096-3642.1990.tb01865.x)
86. Tahara R. 2015 *Structure and development of the avian cranial pneumatic system*. Montreal, Canada: McGill University.
87. Osmólska H. 1985 Antorbital fenestra of archosaurs and its suggested function. *Fortschritte der Zoologie* **30**, 159–162.
88. Witmer LM. 1997 The evolution of the antorbital cavity of archosaurs: a study in soft-tissue reconstruction in the fossil record with an analysis of the function of pneumaticity. *J. Vertebr. Paleontol*. **17**, 1–76. (doi:10.1080/02724634.1997.10011027)
89. Witmer LM, Ridgely RC. 2008 The paranasal air sinuses of predatory and armored dinosaurs (Archosauria: Theropoda and Ankylosauria) and their contribution to cephalic structure. *Anat. Rec.***291**, 1362–1388. (doi:10.1002/ar.20794)
90. Ezcurra MD. 2017 A new early coelophysoid neotheropod from the Late Triassic of Northwestern Argentina. *Ameghiniana* **54**, 506–538. (doi:10.5710/amgh.04.08.2017.3100)